

CERN-EP-2017-292
2018/06/06

CMS-HIG-17-001

Search for lepton flavour violating decays of the Higgs boson to $\mu\tau$ and $e\tau$ in proton-proton collisions at $\sqrt{s} = 13$ TeV

The CMS Collaboration*

Abstract

A search for lepton flavour violating decays of the Higgs boson in the $\mu\tau$ and $e\tau$ decay modes is presented. The search is based on a data set corresponding to an integrated luminosity of 35.9 fb^{-1} of proton-proton collisions collected with the CMS detector in 2016, at a centre-of-mass energy of 13 TeV. No significant excess over the standard model expectation is observed. The observed (expected) upper limits on the lepton flavour violating branching fractions of the Higgs boson are $\mathcal{B}(\text{H} \rightarrow \mu\tau) < 0.25\%$ (0.25%) and $\mathcal{B}(\text{H} \rightarrow e\tau) < 0.61\%$ (0.37%), at 95% confidence level. These results are used to derive upper limits on the off-diagonal $\mu\tau$ and $e\tau$ Yukawa couplings $\sqrt{|Y_{\mu\tau}|^2 + |Y_{\tau\mu}|^2} < 1.43 \times 10^{-3}$ and $\sqrt{|Y_{e\tau}|^2 + |Y_{\tau e}|^2} < 2.26 \times 10^{-3}$ at 95% confidence level. The limits on the lepton flavour violating branching fractions of the Higgs boson and on the associated Yukawa couplings are the most stringent to date.

Published in the Journal of High Energy Physics as doi:10.007/JHEP06(2018)001.

arXiv:1712.07173v3 [hep-ex] 4 Jun 2018

1 Introduction

The discovery of the Higgs boson (H) at the CERN LHC [1–3] has stimulated further precision measurements of the properties of the new particle. A combined study of the 7 and 8 TeV data sets collected by the CMS and ATLAS collaborations shows consistency between the measured couplings of the Higgs boson and the standard model (SM) predictions [4]. However, the constraint on the branching fraction to non-SM decay modes derived from these measurements, $\mathcal{B}(\text{non-SM}) < 34\%$ at 95% confidence level (CL), still allows for a significant contribution from exotic decays [4].

In this paper a search for lepton flavour violating (LFV) decays of the Higgs boson in the $\mu\tau$ and $e\tau$ channels is presented. These decays are forbidden in the SM but occur in many new physics scenarios. These include supersymmetric [5–13], composite Higgs [14, 15], or Randall–Sundrum models [16–18], SM extensions with more than one Higgs boson doublet [19, 20] or with flavour symmetries [21], and many other scenarios [22–36]. The presence of LFV Higgs boson couplings would allow $\tau \rightarrow \mu$ and $\tau \rightarrow e$ to proceed via a virtual Higgs boson [37, 38]. Consequently the experimental limits on rare τ lepton decays, such as $\tau \rightarrow e\gamma$ and $\tau \rightarrow \mu\gamma$ [39], provide upper limits on $\mathcal{B}(H \rightarrow \mu\tau)$ and $\mathcal{B}(H \rightarrow e\tau)$ [40, 41] of $\mathcal{O}(10\%)$. Measurements of the electron and muon magnetic moments, and exclusion limits on the electric dipole moment of the electron also provide complementary constraints [42]. The LFV Higgs boson decay to μe is strongly constrained by the $\mu \rightarrow e\gamma$ limit, $\mathcal{B}(H \rightarrow e\mu) < \mathcal{O}(10^{-9})$ [43].

The CMS experiment published the first direct search for $H \rightarrow \mu\tau$ [44], followed by searches for $H \rightarrow e\tau$ and $H \rightarrow e\mu$ decays [45], using proton-proton (pp) collision data corresponding to an integrated luminosity of 19.7 fb^{-1} at a centre-of-mass energy of 8 TeV. A small excess of data with respect to the SM background-only hypothesis at $m_H = 125 \text{ GeV}$ was observed in the $H \rightarrow \mu\tau$ channel, with a significance of 2.4 standard deviations (σ), and the best fit for the branching fraction was found to be $\mathcal{B}(H \rightarrow \mu\tau) = (0.84_{-0.37}^{+0.39})\%$. A constraint was set on the observed (expected) branching fraction $\mathcal{B}(H \rightarrow \mu\tau) < 1.51\%$ (0.75%) at 95% CL. No excess of events over the estimated background was observed in the $H \rightarrow e\tau$ or $H \rightarrow e\mu$ channels, and observed (expected) upper limits on the branching fractions $\mathcal{B}(H \rightarrow e\tau) < 0.69\%$ (0.75%) and $\mathcal{B}(H \rightarrow e\mu) < 0.035\%$ (0.048%) at 95% CL were set. The ATLAS Collaboration reported searches for $H \rightarrow e\tau$ and $H \rightarrow \mu\tau$ using pp collision data at a centre-of-mass energy of 8 TeV, finding no significant excess of events over the background expectation, and set observed (expected) limits of $\mathcal{B}(H \rightarrow \mu\tau) < 1.43\%$ (1.01%) and $\mathcal{B}(H \rightarrow e\tau) < 1.04\%$ (1.21%) at 95% CL [46, 47].

The search described in this paper is performed in four decay channels, $H \rightarrow \mu\tau_h$, $H \rightarrow \mu\tau_e$, $H \rightarrow e\tau_h$, $H \rightarrow e\tau_\mu$, where τ_h , τ_e , and τ_μ correspond to the hadronic, electronic, and muonic decay channels of τ leptons, respectively. The decay channels $H \rightarrow e\tau_e$ and $H \rightarrow \mu\tau_\mu$ are not considered because of the large background contribution from Z boson decays. The expected final state signatures are very similar to those for the SM $H \rightarrow \tau\tau$ decays, studied by CMS [48–50] and ATLAS [51], but with some significant kinematic differences. The electron (muon) in the LFV $H \rightarrow e(\mu)\tau$ decay is produced promptly, and tends to have a larger momentum than in the SM $H \rightarrow \tau_{e(\mu)}\tau_h$ decay. The search reported in this paper improves upon the sensitivity of the earlier CMS searches [44, 45] by using a boosted decision trees (BDT) discriminator to distinguish signal from background events. A separate analysis, similar in strategy to the previous CMS publications, is performed as cross check. The results of both strategies are reported in this paper.

This paper is organized as follows. After a description of the CMS detector (Section 2) and of the collision data and simulated samples used in the analyses (Section 3), the event reconstruc-

tion is described in Section 4. The event selection is described separately for the two Higgs boson decay modes $H \rightarrow e\tau$ and $H \rightarrow \mu\tau$ in Section 5. The backgrounds, which are common to all channels but with different rates in each, are described in Section 6. The systematic uncertainties are described in Section 7 and the results are then presented in Section 8.

2 The CMS detector

The central feature of the CMS apparatus is a superconducting solenoid of 6 m internal diameter, providing a magnetic field of 3.8 T. Within the solenoid volume are a silicon pixel and strip tracker, a lead tungstate crystal electromagnetic calorimeter (ECAL), and a brass and scintillator hadron calorimeter (HCAL), each composed of a barrel and two endcap sections. Forward calorimeters extend the pseudorapidity (η) coverage provided by the barrel and endcap detectors. Muons are detected in gas-ionization chambers embedded in the steel flux-return yoke outside the solenoid. The two-level CMS trigger system selects events of interest for permanent storage [52]. The first trigger level, composed of custom hardware processors, uses information from the calorimeters and muon detectors to select events at a rate of around 100 kHz within a time interval of less than 4 μ s. The software algorithms of the high-level trigger, executed on a farm of commercial processors, reduce the event rate to about 1 kHz using information from all detector subsystems. A detailed description of the CMS detector, together with a definition of the coordinate system used and the relevant kinematic variables, can be found in Ref. [53].

3 Collision data and simulated events

The analyses presented here use samples of pp collisions collected in 2016 by the CMS experiment at the LHC at a centre-of-mass energy of $\sqrt{s} = 13$ TeV, corresponding to an integrated luminosity of 35.9 fb^{-1} . Isolated single muon triggers are used to collect the data samples in the $H \rightarrow \mu\tau$ search. Triggers requiring a single isolated electron, or a combination of an electron and a muon, are used in the $H \rightarrow e\tau_h$ and $H \rightarrow e\tau_\mu$ channels, respectively. Simulated samples of signal and background events are produced with several event generators. The Higgs bosons are produced in pp collisions predominantly by gluon fusion (ggH) [54], but also by vector boson fusion (VBF) [55], and in association with a W or Z boson [56]. The ggH and VBF Higgs boson samples are generated with POWHEG 2.0 [57–62] while the MINLO HVJ [63] extension of POWHEG 2.0 is used for the WH and ZH simulated samples. The MG5_aMC@NLO [64] generator is used for Z + jets and W + jets processes. They are simulated at leading order (LO) with the MLM jet matching and merging [65]. Diboson production is simulated at next-to-LO (NLO) using MG5_aMC@NLO generator with the FxFx jet matching and merging [66], whereas POWHEG 2.0 and 1.0 are used for $t\bar{t}$ and single top quark production, respectively. The POWHEG and MADGRAPH generators are interfaced with PYTHIA 8.212 [67] for parton showering, fragmentation, and decays. The PYTHIA parameters for the underlying event description are set to the CUETP8M1 tune [68]. Due to the high instantaneous luminosities attained during data taking, many events have multiple pp interactions per bunch crossing (pileup). The effect is taken into account in simulated samples, by generating concurrent minimum bias events. All simulated samples are weighted to match the pileup distribution observed in data, that has an average of approximately 27 interactions per bunch crossing. The CMS detector response is modelled using GEANT4 [69].

4 Event reconstruction

The global event reconstruction is performed using a particle-flow (PF) algorithm, which reconstructs and identifies each individual particle with an optimized combination of all subdetector information [70]. In this process, the identification of the particle type (photon, electron, muon, charged or neutral hadron) plays an important role in the determination of the particle direction and energy. The primary pp vertex of the event is identified as the reconstructed vertex with the largest value of summed physics-object p_T^2 , where p_T is the transverse momentum. The physics objects are returned by a jet finding algorithm [71, 72] applied to all charged tracks associated with the vertex, plus the corresponding associated missing transverse momentum.

A muon is identified as a track in the silicon detectors, consistent with the primary pp vertex and with either a track or several hits in the muon system, associated with an energy deposit in the calorimeters compatible with the expectations for a muon [70, 73]. Identification is based on the number of spacial points measured in the tracker and in the muon system, the track quality and its consistency with the event vertex location. The energy is obtained from the corresponding track momentum.

An electron is identified as a charged particle track from the primary pp vertex in combination with one or more ECAL energy clusters. These clusters correspond to the track extrapolation to the ECAL and to possible bremsstrahlung photons emitted when interacting with the material of the tracker [74]. Electron candidates are accepted in the range $|\eta| < 2.5$, with the exception of the region $1.44 < |\eta| < 1.57$ where service infrastructure for the detector is located. They are identified using a multivariate (MVA) discriminator that combines observables sensitive to the amount of bremsstrahlung along the electron trajectory, the geometrical and momentum matching between the electron trajectory and associated clusters as well as various shower shape observables in the calorimeters. Electrons from photon conversions are removed. The energy of electrons is determined from a combination of the track momentum at the primary vertex, the corresponding ECAL cluster energy, and the energy sum of all bremsstrahlung photons attached to the track.

Hadronically decaying τ leptons are reconstructed and identified using the hadrons-plus-strips (HPS) algorithm [75, 76]. The reconstruction starts from a jet and searches for the products of the main τ lepton decay modes: one charged hadron and up to two neutral pions, or three charged hadrons. To improve the reconstruction efficiency in the case of conversion of the photons from neutral-pion decay, the algorithm considers the PF photons and electrons from a strip along the azimuthal direction ϕ . The charges of all the PF objects from tau lepton decay, except for the electrons from neutral pions, are summed to reconstruct the tau lepton charge. An MVA discriminator, based on the information of the reconstructed tau lepton and of the charged particles in a cone around it, is used to reduce the rate for quark- and gluon-initiated jets identified as τ candidates. The working point used in the analysis has an efficiency of about 60% for a genuine τ_h , with approximately a 0.5% misidentification rate for quark and gluon jets [76]. Additionally, muons and electrons misidentified as tau leptons are rejected using a dedicated set of selection criteria based on the consistency between the measurements in the tracker, calorimeters, and muon detectors. The specific identification criteria depend on the final state studied and on the background composition. The tau leptons that decay to muons and electrons are reconstructed as prompt muons and electrons as described above.

Charged hadrons are identified as charged particle tracks from the primary pp vertex neither reconstructed as electrons nor as muons nor as τ leptons. Neutral hadrons are identified as HCAL energy clusters not assigned to any charged hadron, or as ECAL and HCAL energy excesses with respect to the expected charged-hadron energy deposit. All the PF candidates are

clustered into hadronic jets using the infrared and collinear safe anti- k_T algorithm [71], implemented in the FASTJET package [77], with a distance parameter of 0.4. The jet momentum is determined as the vector sum of all particle momenta in this jet, and is found in the simulation to be on average within 10% of the true momentum over the whole p_T spectrum and detector acceptance. An offset correction is applied to jet energies to take into account the contribution from pileup [78]. Jet energy corrections are derived from the simulation, and are confirmed with in situ measurements of the energy balance of dijet, multijet, photon + jet, and Z + jet events [79]. The variable $\Delta R = \sqrt{(\Delta\eta)^2 + (\Delta\phi)^2}$ is used to measure the separation between reconstructed objects in the detector. Any jet within $\Delta R = 0.4$ of the identified leptons is removed.

Jets misidentified as electrons, muons, or tau leptons are suppressed by imposing isolation requirements. The muon (electron) isolation is measured relative to its p_T^ℓ ($\ell = e, \mu$), by summing over the p_T of PF particles in a cone with $\Delta R = 0.4$ (0.3) around the lepton:

$$I_{\text{rel}}^\ell = \left(\sum p_T^{\text{charged}} + \max \left[0, \sum p_T^{\text{neutral}} + \sum p_T^\gamma - p_T^{\text{PU}}(\ell) \right] \right) / p_T^\ell,$$

where p_T^{charged} , p_T^{neutral} , and p_T^γ indicate the p_T of a charged particle, a neutral particle, and a photon within the cone, respectively. The neutral contribution to isolation from pileup, $p_T^{\text{PU}}(\ell)$, is estimated from the area of the jet and the average energy density of the event [80, 81] for the electron or from the sum of transverse momenta of charged hadrons not originating from the primary vertex scaled by a factor of 0.5 for the muons. The charged contribution to isolation from pileup is rejected requiring the tracks to originate from the primary vertex.

All the reconstructed particles in the event are used to estimate the missing transverse momentum, \vec{p}_T^{miss} , which is defined as the negative of the vector \vec{p}_T sum of all identified PF objects in the event [82]. Its magnitude is referred to as p_T^{miss} .

The transverse mass $M_T(\ell)$ is a variable formed from the lepton momentum and the missing transverse momentum vectors: $M_T(\ell) = \sqrt{2|\vec{p}_T^\ell||\vec{p}_T^{\text{miss}}|(1 - \cos \Delta\phi_{\ell-p_T^{\text{miss}}})}$, where $\Delta\phi_{\ell-p_T^{\text{miss}}}$ is the angle in the transverse plane between the lepton and the missing transverse momentum. It is used to discriminate the Higgs boson signal candidates from the W + jets background. The collinear mass, M_{col} , provides an estimate of m_H using the observed decay products of the Higgs boson candidate. It is reconstructed using the collinear approximation based on the observation that, since $m_H \gg m_\tau$, the τ lepton decay products are highly Lorentz boosted in the direction of the τ candidate [83]. The neutrino momenta can be approximated to have the same direction as the other visible decay products of the τ ($\vec{\tau}^{\text{vis}}$) and the component of the \vec{p}_T^{miss} in the direction of the visible τ lepton decay products is used to estimate the transverse component of the neutrino momentum ($p_T^{\nu, \text{est}}$). The collinear mass can then be derived from the visible mass of the τ - μ or τ -e system (M_{vis}) as $M_{\text{col}} = M_{\text{vis}} / \sqrt{x_\tau^{\text{vis}}}$, where x_τ^{vis} is the fraction of energy carried by the visible decay products of the τ ($x_\tau^{\text{vis}} = p_T^{\vec{\tau}^{\text{vis}}} / (p_T^{\vec{\tau}^{\text{vis}}} + p_T^{\nu, \text{est}})$), and M_{vis} is the invariant mass of the visible decay products.

5 Event selection

The signal contains a prompt isolated lepton, μ or e , along with an oppositely charged isolated lepton of different flavour (τ_μ, τ_e or τ_h). In each decay mode a loose selection of this signature is defined first. The events are then divided into categories within each sample according to the number of jets in the event. This is designed to enhance the contribution of different Higgs boson production mechanisms. The jets are required to have $p_T > 30$ GeV and $|\eta| < 4.7$.

The 0-jet category enhances the ggH contribution, while the 1-jet category enhances ggH production with initial-state radiation. The 2-jet ggH category has a further requirement that the invariant mass of the two jets $M_{jj} < 550$ GeV while the 2-jet VBF category with the requirement $M_{jj} \geq 550$ GeV enhances the VBF contribution. The threshold on M_{jj} has been optimized to give the best expected exclusion limits. The definition of the categories is the same in all the channels except in the $H \rightarrow e\tau$ channels where the M_{jj} threshold is 500 GeV, which optimizes the expected limits for this channel.

After the loose selection, a binned likelihood is used to fit the distribution of a BDT discriminator for the signal and the background contributions. This is referred to as the BDT fit analysis. As a cross-check an analysis using a tighter set of selection criteria is also presented. In this case, selection requirements are placed on the kinematic variables and a fit is performed to the M_{col} distribution. This is referred to as the M_{col} fit analysis. Requirements on additional kinematic variables such as $M_T(\ell)$ are chosen to obtain the most stringent expected limits. The lepton p_T has been excluded from this optimization to avoid biasing the selection toward energetic leptons that sculpt the background M_{col} distribution to mimic the signal peak. This effect would reduce the shape discrimination power of the signal extraction procedure.

5.1 $H \rightarrow \mu\tau_h$

The loose selection begins by requiring an isolated μ and an isolated τ_h of opposite charge and separated by $\Delta R > 0.3$. The muon candidate is required to have $p_T^\mu > 26$ GeV, $|\eta^\mu| < 2.4$ and $I_{\text{rel}}^\mu < 0.15$. The hadronic tau candidate is required to have $p_T^{\tau_h} > 30$ GeV and $|\eta^{\tau_h}| < 2.3$. The isolation requirement for the τ_h candidates is included in the MVA used for the HPS identification algorithm described in Section 4. Events with additional e, μ or τ_h candidates are vetoed. Events with at least one jet identified by the combined secondary vertex b-tagging algorithm [84] as arising from a b quark, are also vetoed in order to suppress the $t\bar{t}$ background. The tighter selection used for the M_{col} fit analysis further requires $M_T(\tau_h) < 105$ GeV in the 0-, 1- and 2-jet ggH categories, and $M_T(\tau_h) < 85$ GeV in the 2-jet VBF category. The selections are summarized in Table 1.

A BDT is trained after the loose selection combining all categories. The signal training sample used is a mixture of simulated ggH and VBF events, weighted according to their respective SM production cross sections. The background training sample is a set of collision events with misidentified leptons, as this is the dominant background in this channel. The leptons are required to satisfy the same kinematic selection of the signal sample, be like-sign and not isolated in order to select an orthogonal data set to the signal sample, and yet have the same kinematic properties. The input variables to the BDT are: p_T^μ , $p_T^{\tau_h}$, M_{col} , p_T^{miss} , $M_T(\tau_h)$, $\Delta\eta(\mu, \tau_h)$, $\Delta\phi(\mu, \tau_h)$, and $\Delta\phi(\tau_h, \vec{p}_T^{\text{miss}})$. The neutrino in the τ lepton decay leads to the presence of significant missing momentum motivating the inclusion of the p_T^{miss} variables. The neutrino is also approximately collinear with the visible τ decay products while the two leptons tend to be azimuthally opposite leading to the inclusion of the $\Delta\phi$ variables. The BDT input variables are shown for signal and background in Fig. 1.

5.2 $H \rightarrow \mu\tau_e$

The loose selection begins by requiring an isolated μ and an isolated e of opposite charge and separated by $\Delta R > 0.3$. The muon candidate is required to have $p_T^\mu > 26$ GeV, $|\eta^\mu| < 2.4$, and $I_{\text{rel}}^\mu < 0.15$. The electron candidate is required to have $p_T^e > 10$ GeV, $|\eta^e| < 2.4$, and $I_{\text{rel}}^e < 0.1$. Events with additional e, μ or τ_h candidates, or with at least one b-tagged jet are vetoed.

The tighter selection used in the M_{col} fit analysis requires $p_T^\mu > 30$ GeV for the 0-jet category

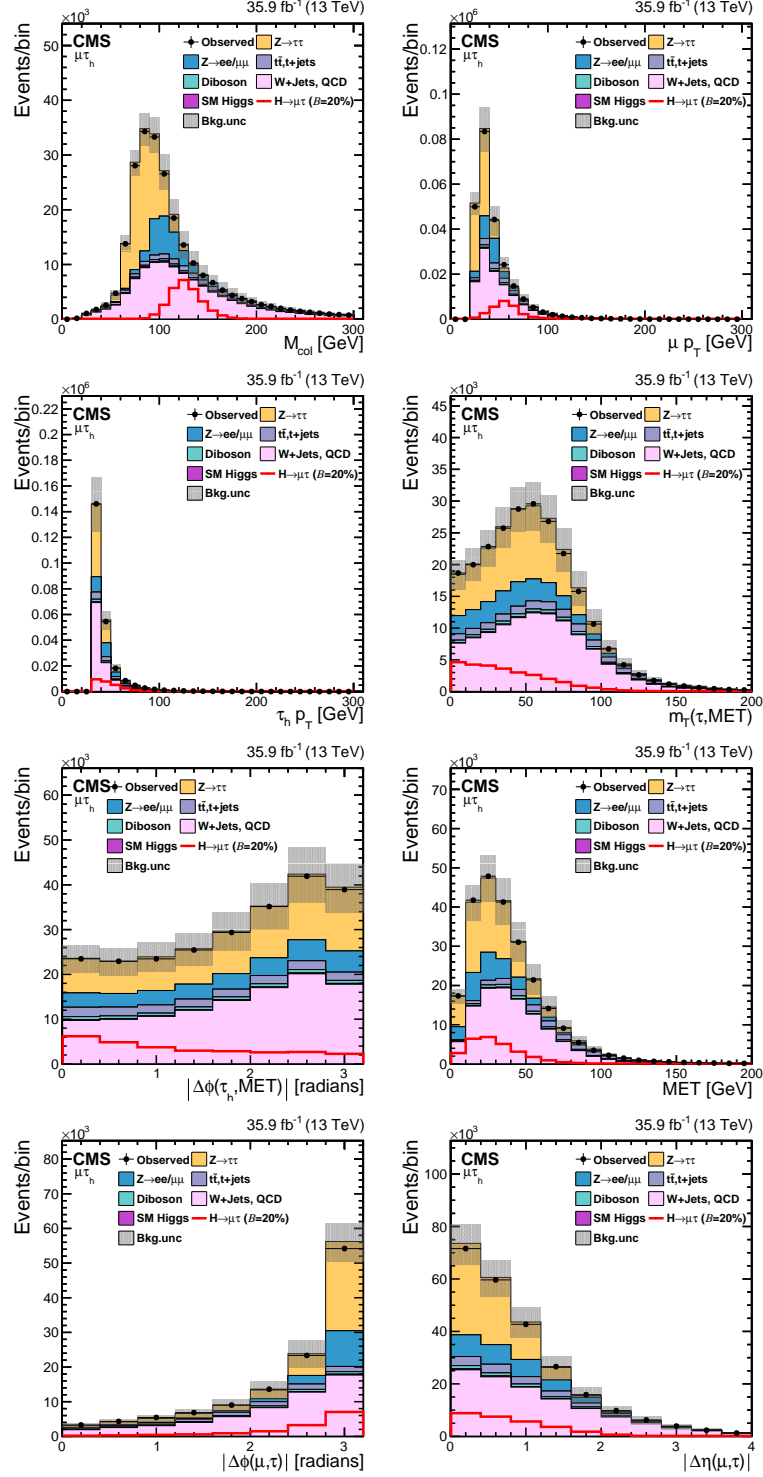


Figure 1: Distributions of the input variables to the BDT for the $H \rightarrow \mu\tau_h$ channel. The background from SM Higgs boson production is small and not visible in the plots.

and $p_T^\mu > 26$ GeV in the other categories. In the 0-, 1-, 2-jet ggH and 2-jet VBF categories, $M_T(\mu)$ is required to be greater than 60, 40, 15, and 15 GeV respectively. A requirement is made on the azimuthal angle between the electron and the \vec{p}_T^{miss} : $\Delta\phi(e, \vec{p}_T^{\text{miss}}) < 0.7, 0.7, 0.5, 0.3$ for the 0-, 1-, 2-jet ggH, and 2-jet VBF categories, respectively. In the 0- and 1-jet categories it is further required that $\Delta\phi(e, \mu) > 2.5$ and 1.0, respectively. The selections are summarized in Table 1.

A BDT is trained after the loose selection, combining all categories. The background is a mixed sample of $t\bar{t}$ and $Z \rightarrow \ell\ell$ ($\ell = e, \mu, \tau$) events weighted by their production cross-sections. The $t\bar{t}$ background is the dominant background in this channel for the 2-jet category and also very significant in the 1-jet category. It has many kinematic characteristics in common with the other backgrounds, such as diboson and single top. The $Z \rightarrow \ell\ell$ background is the dominant background in 0- and 1-jet category. The input variables to the BDT are: p_T^μ , p_T^e , M_{col} , $M_T(\mu)$, $M_T(e)$, $\Delta\phi(e, \mu)$, $\Delta\phi(e, \vec{p}_T^{\text{miss}})$, and $\Delta\phi(\mu, \vec{p}_T^{\text{miss}})$. The distributions of these variables are shown in Fig. 2.

Table 1: Event selection criteria for the kinematic variables for the $H \rightarrow \mu\tau$ channels.

Variable	$H \rightarrow \mu\tau_h$				$H \rightarrow \mu\tau_e$				
	0 jet	1 jet	2 jet		0 jet	1 jet	2 jet		
			ggH	VBF			ggH	VBF	
M_{jj}	[GeV]	—	—	<550	≥550	—	—	<550	≥550
p_T^e	[GeV]		—				>10		
p_T^μ	[GeV]		>26				>26		
$p_T^{\tau_h}$	[GeV]		>30				—		
$ \eta^e $			—				<2.4		
$ \eta^\mu $			<2.4				<2.4		
$ \eta^{\tau_h} $			<2.3				—		
I_{rel}^e			—				<0.1		
I_{rel}^μ			<0.15				<0.15		
M_{col} fit selection									
p_T^μ	[GeV]		—			>30	—	—	—
$M_T(\mu)$	[GeV]		—			>60	>40	>15	>15
$M_T(\tau_h)$	[GeV]	<105	<105	<105	<85			—	
$\Delta\phi(e, \vec{p}_T^{\text{miss}})$	[radians]		—			<0.7	<0.7	<0.5	<0.3
$\Delta\phi(e, \mu)$	[radians]		—			>2.5	>1.0	—	—

5.3 $H \rightarrow e\tau_h$

The loose selection begins by requiring an isolated e and an isolated τ_h candidate of opposite charge, separated by $\Delta R > 0.5$. The e candidate is required to have $p_T^e > 26$ GeV, $|\eta^e| < 2.1$, and $I_{\text{rel}}^e < 0.1$. The τ_h candidate is required to have $p_T^{\tau_h} > 30$ GeV and $|\eta^{\tau_h}| < 2.3$. Events with additional e , μ or τ_h candidates are vetoed. No veto is made on the number of b-tagged jets as the $t\bar{t}$ contribution is small. The additional selection used for the M_{col} fit analysis further requires that $M_T(\tau_h) < 60$ GeV. The selections are summarized in Table 2. A BDT is trained after the loose selection. The same training samples as for the $H \rightarrow \mu\tau_h$ channel are used, except with an electron rather than a muon. The input variables to the BDT are also the same except for the addition of the visible mass, M_{vis} , and the removal of p_T^{miss} . The relative composition of the backgrounds in the $H \rightarrow e\tau_h$ channel is different from the $H \rightarrow \mu\tau_h$ channel, in particular the $Z \rightarrow ee + \text{jets}$ background is larger in comparison to the $Z \rightarrow \mu\mu + \text{jets}$, which leads to this change of variables.

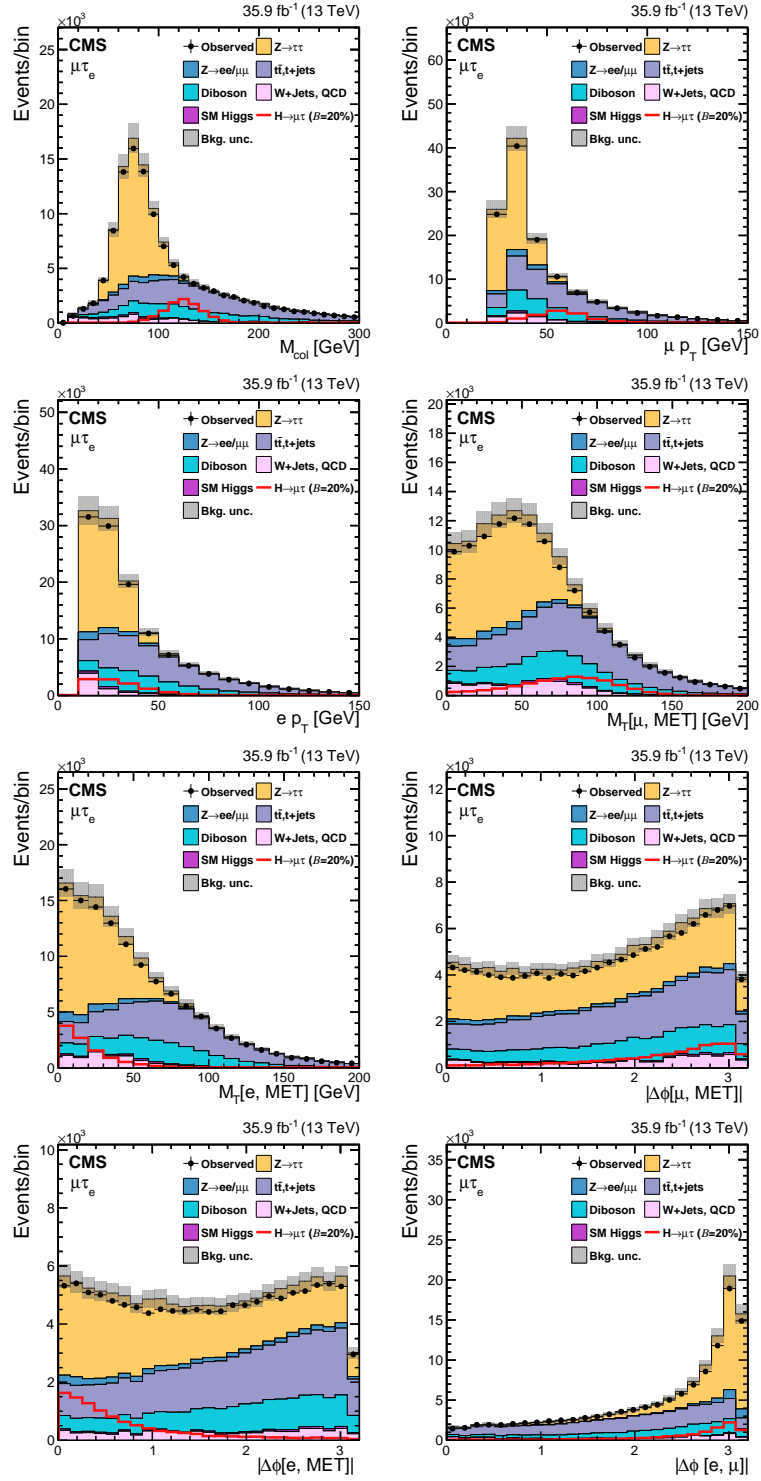


Figure 2: Distributions of the input variables to the BDT for the $H \rightarrow \mu\tau_e$ channel.

5.4 $H \rightarrow e\tau_\mu$

The loose selection begins by requiring an isolated e and an isolated μ candidate with opposite charge, separated by $\Delta R > 0.4$. The e candidate is required to have $p_T^e > 24$ GeV, $|\eta^e| < 2.1$, and $I_{\text{rel}}^e < 0.1$. The μ candidate is required to have $p_T^\mu > 10$ GeV, $|\eta^\mu| < 2.4$, and $I_{\text{rel}}^\mu < 0.15$. Events with additional e , μ or τ_h candidates, or with at least one b-tagged jet are vetoed.

The tighter selection used in the M_{col} fit analysis further requires $\Delta\phi(e, \vec{p}_T^{\text{miss}}) < 1.0$ and $M_T(e) > 60$ GeV. The large $t\bar{t}$ background is further reduced by requiring $p_\zeta - 0.85 p_\zeta^{\text{vis}} > -60$ GeV. This topological selection is based on the projections

$$p_\zeta = (\vec{p}_T^e + \vec{p}_T^\mu + \vec{p}_T^{\text{miss}}) \frac{\vec{\zeta}}{|\vec{\zeta}|} \quad \text{and} \quad p_\zeta^{\text{vis}} = (\vec{p}_T^e + \vec{p}_T^\mu) \frac{\vec{\zeta}}{|\vec{\zeta}|}$$

on the axis $\vec{\zeta}$ bisecting the directions of the electron, \vec{p}_T^e , and of the muon, \vec{p}_T^μ . This selection criterion is highly efficient in rejecting background as the \vec{p}_T^{miss} is oriented in the direction of the visible τ decay products in signal events. The selection criteria are summarized in Table 2.

A BDT is trained after the loose selection. It uses the same input variables as for the $H \rightarrow \mu\tau_e$ channel with the addition of the visible mass, M_{vis} , and the removal of $M_T(e)$. The background used for the training is a sample of simulated $t\bar{t}$ events.

Table 2: Event selection criteria for the kinematic variables for the $H \rightarrow e\tau$ channels.

Variable	$H \rightarrow e\tau_h$				$H \rightarrow e\tau_\mu$				
	0 jet	1 jet	2 jet		0 jet	1 jet	2 jet		
			ggH	VBF			ggH	VBF	
M_{jj}	[GeV]	—	—	<500	>500	—	—	<500	>500
p_T^e	[GeV]			>26				>24	
p_T^μ	[GeV]			—				>10	
$p_T^{\tau_h}$	[GeV]			>30				—	
$ \eta^e $				<2.1				<2.1	
$ \eta^\mu $				—				<2.4	
$ \eta^{\tau_h} $				<2.3				—	
I_{rel}^e				<0.15				<0.1	
I_{rel}^μ				—				<0.1	
M_{col} fit selection									
$M_T(\tau_h)$	[GeV]			<60				—	
$M_T(e)$	[GeV]			—				>60	
$\Delta\phi(e, \vec{p}_T^{\text{miss}})$	[radians]			—				<1.0	
$p_\zeta - 0.85 p_\zeta^{\text{vis}}$	[GeV]			—				> -60	

6 Background estimation

The main background processes are $Z \rightarrow \tau\tau$, in which the μ or e arises from a τ decay, and W +jets and QCD multijet production where one or more of the jets are misidentified as leptons. Other backgrounds come from processes in which the lepton pair is produced from the weak decays of quarks and vector bosons. These include $t\bar{t}$ pairs, Higgs boson production ($H \rightarrow \tau\tau, WW$), WW , WZ , and ZZ . There are also smaller contributions from $W\gamma^{(*)}$ + jets processes, single top quark production, and $Z \rightarrow \ell\ell$ ($\ell = e, \mu$). All the backgrounds are estimated from simulated samples with the exception of the misidentified-lepton backgrounds

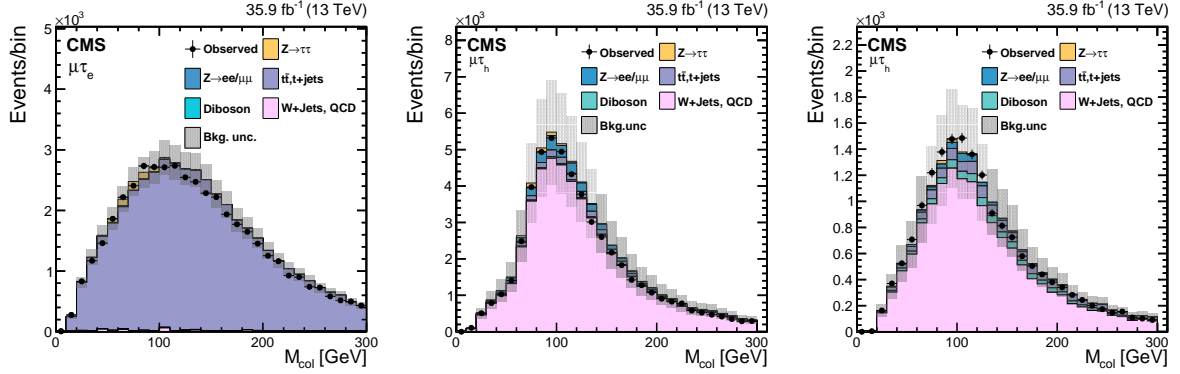


Figure 3: M_{col} distribution in $t\bar{t}$ enriched (left), like-sign lepton (central), and $W + \text{jets}$ enriched (right) control samples defined in the text. The distributions include both statistical and systematic uncertainties.

that are estimated from data with either fully data-driven or semi data-driven methods. These techniques are described in detail below. The background estimate is validated with control regions designed to have enhanced contributions from the dominant backgrounds.

The $Z \rightarrow \ell\ell$ background is estimated from simulation. A reweighting is applied to correct the generator-level $Z p_T$ and $m_{\ell\ell}$ distributions in LO MG5_aMC@NLO samples to reduce the shape discrepancy between collision data and simulation. The reweighting factors are extracted from a $Z \rightarrow \mu\mu$ control region and are applied to both $Z \rightarrow \mu\mu$ and $Z \rightarrow ee$ simulated samples in bins of $Z p_T$ and $m_{\ell\ell}$. Additional corrections for $\mu \rightarrow \tau_h$ and $e \rightarrow \tau_h$ misidentification rates are applied when the reconstructed τ_h candidate is matched to a muon or an electron, respectively, at the generator level. These corrections are measured in $Z \rightarrow \ell\ell$ events and depend on the lepton η . The $t\bar{t} + \text{jets}$ background is particularly important in the $e\mu$ final state. A correction based on the generated p_T of the top quark and antiquark is applied to the simulation to match the p_T distribution observed in a $t\bar{t}$ sample from collision data. The background estimation for this contribution is validated in a $t\bar{t}$ enriched control sample. It is defined by requiring the loose selection for these channels but with the additional requirement that at least one of the jets is b-tagged. Figure 3 (left) shows the data compared to the background estimation for this control sample in the $H \rightarrow \mu\tau_e$ channel. The same samples are used in the $H \rightarrow e\tau_\mu$ channel and show similar agreement.

The Higgs boson production contributes a small but non-negligible background. It arises predominantly from $H \rightarrow \tau\tau$ but also from $H \rightarrow WW$ decays and peaks at lower values of M_{col} than the signal, because of additional neutrinos in the decays. The event selection described in Section 5 uses a BDT discriminator that combines M_{col} with a set of other kinematic variables. The Higgs boson background also peaks below the signal in the distribution of the BDT discriminator output.

Jets misidentified as leptons are a source of background arising from two sources, $W + \text{jets}$ and QCD multijet events. In $W + \text{jets}$ background events, one lepton candidate is a real lepton from the W boson decay and the other is a jet misidentified as a lepton. In QCD multijet events, both lepton candidates are misidentified jets. In each of the four channels for this analysis ($\mu\tau_h, e\tau_h, \mu\tau_e, e\tau_\mu$), the misidentified-lepton background has been estimated using purely data-driven methods. In the $\mu\tau_e$ and $e\tau_\mu$ channels it is also estimated using a technique, called semi data-driven, partially based on control samples in data and partially on simulation. It has been used previously in the SM $H \rightarrow \tau\tau$ analysis [50]. The misidentified $W + \text{jets}$ background is estimated from simulation and the QCD background with data. The two techniques give

consistent results; the semi data-driven technique is chosen for the leptonically decaying tau channels as the fully data-driven technique is limited by the reduced size of the sample.

Fully data-driven technique

The misidentified lepton background is estimated from collision data samples. The misidentification rates are evaluated with independent $Z + \text{jets}$ data sets and then applied to a control region, orthogonal to the signal region, to estimate the misidentified background in the signal region. This control region is obtained by relaxing the signal selection requirements, typically isolation, and excluding events passing the final selection. The probabilities with which jets are misidentified as e (f_e), μ (f_μ), or τ_h (f_τ), are estimated using events with a Z boson candidate plus one jet that can be misidentified as a lepton. The Z boson candidate is formed from two muons with $p_T > 26$ GeV, $|\eta| < 2.4$, and $I_{\text{rel}}^\ell < 0.15$ (0.25) for the jet $\rightarrow \tau_h, \mu$ (jet $\rightarrow e$) misidentification rate. The muons are required to have opposite charge and their invariant mass ($M_{\mu\mu}$) must satisfy $70 < M_{\mu\mu} < 110$ GeV. The contribution from diboson events, where the third lepton candidate corresponds to a genuine lepton, is subtracted using simulation. Two $Z + \text{jets}$ samples are defined: the signal-like one, in which the jet satisfies the same lepton selection criteria used in the $H \rightarrow e\tau$ or $H \rightarrow \mu\tau$ selections, and the background-enriched $Z + \text{jets}$ sample with relaxed lepton identification on the jet but excluding events selected in the signal-like sample. The requirements for the third lepton candidate vary depending on the lepton flavour. The two samples are used to estimate f_e, f_μ and f_τ which are obtained as

$$f_i = \frac{N_i(\text{Z + jets signal-like})}{N_i(\text{Z + jets background-enriched}) + N_i(\text{Z + jets signal-like})},$$

where $N_i(\text{Z + jets signal-like})$ is the number of events with a third lepton candidate that passes the signal-like sample selection, $N_i(\text{Z + jets background-enriched})$ is the number of events in the background-enriched sample and $i = e, \mu$ or τ . The lepton selection criteria for the signal are given in Table 1 and 2. The background-enriched lepton selection used to estimate the misidentified μ and e contribution requires an isolation of $0.15 < I_{\text{rel}}^\ell < 0.25$ and $0.1 < I_{\text{rel}}^\ell < 0.5$, respectively. In both cases the misidentification rate is computed as a function of the lepton p_T . The lepton selection for the τ_h background-enriched sample requires that the tau candidates are identified using a loose HPS working point but are not identified by the tight working point used for the signal selection. The loose and the tight working points have an efficiency of 75% and 60% for genuine τ_h candidates, respectively. The misidentification rates show a p_T dependence that varies with the τ decay mode and $|\eta|$. The misidentification rates are thus obtained as a function of p_T for the different decay modes and $|\eta|$ regions ($|\eta| < 1.5$ or $|\eta| > 1.5$).

The final misidentified lepton background in the signal region for the two analyses (BDT and M_{col} fit) is obtained from background-enriched signal-like samples (LFV background-enriched, type i), where the lepton i ($i = e, \mu$ or τ) passes the identification and isolation criteria used for the $Z + \text{jets}$ background-enriched sample but not those defining the $Z + \text{jets}$ signal-like sample, but otherwise uses the same selection as the signal. To estimate the misidentified lepton background in the signal sample, each event in this LFV background-enriched sample of type i is weighted by a factor $f_i/(1 - f_i)$, depending on the lepton p_T for electrons and muons or on p_T, η , and decay mode for the τ lepton candidates. Both background yield and shape distributions are thus estimated. Double-counted events with two misidentified leptons are subtracted. For example, events with a misidentified μ (e) and a misidentified τ_h are subtracted in the $H \rightarrow \mu\tau_h$ ($H \rightarrow e\tau_h$) channel using a weight $f_\tau f_\ell / [(1 - f_\tau)(1 - f_\ell)]$ (where $\ell = \mu$ or e) applied to the events of a LFV background-enriched sample defined requiring both leptons to

pass the identification and isolation criteria used for the $Z + \text{jets}$ background-enriched sample but not those defining the $Z + \text{jets}$ signal-like sample.

The background estimation is validated in a like-sign sample applying the misidentification rate f_i to events selected inverting the charge requirement of the lepton pair in both the background-enriched and the signal-like samples. It is performed after the loose selection described in Section 5. Figure 3 (central) shows the data compared to the background estimation in the like-sign control region for the $H \rightarrow \mu\tau_h$ channel. The like-sign selection enhances the misidentified lepton background and there is good agreement in the control sample. The background estimation can also be validated in a W boson enriched control sample. This data sample is obtained by applying the signal sample requirements and $M_T(\ell) > 60 \text{ GeV}$ ($\ell = e$ or μ) and $M_T(\tau_h) > 80 \text{ GeV}$. Figure 3 (right) shows the data compared to the background estimation in the W enriched sample for the $H \rightarrow \mu\tau_h$ channel. The same samples are used in the $H \rightarrow e\tau_h$ channel with similar agreement.

Semi data-driven technique

The $W + \text{jets}$ background contribution to the misidentified-lepton background is estimated with simulated samples. The QCD multijet contribution is estimated with like-sign collision data events that pass the signal requirement. The expected yield from non-QCD processes is subtracted using simulation. The resulting sample is then rescaled to account for the differences between the composition in the like- and opposite-sign samples. The scaling factors are extracted from QCD multijet enriched control samples, composed of events with the lepton candidates satisfying inverted isolation requirements as illustrated in Ref. [50]. This technique is chosen for the leptonically decaying tau channels as the size of the samples allows a more precise background description.

7 Systematic uncertainties

The systematic uncertainties affect the normalization and the shape of the distributions of the different processes, and arise from either experimental or theoretical sources. They are summarized in Table 3. The uncertainties in the lepton (e, μ, τ_h) selection including the trigger, identification, and isolation efficiencies are estimated using tag-and-probe measurements in collision data sets of Z bosons decaying to $ee, \mu\mu, \tau_\mu\tau_h$ [73–76, 86]. The b tagging efficiency in the simulation is adjusted to match the efficiency measured in data. The uncertainty in this measurement is taken as the systematic uncertainty. The uncertainties on the $Z \rightarrow ee, Z \rightarrow \mu\mu, Z \rightarrow \tau\tau, WW, ZZ, W\gamma, t\bar{t}$, and single top production background contributions arise predominantly from the uncertainties in the measured cross sections of these processes. The uncertainties in the estimate of the misidentified-lepton backgrounds ($\mu \rightarrow \tau_h, e \rightarrow \tau_h, \text{jet} \rightarrow \tau_h, \mu, e$) are extracted from the validation tests in control samples, described in Section 6.

Shape and normalization uncertainties arising from the uncertainty in the jet energy scale are computed by propagating the effect of altering each source of jet energy scale uncertainty by one standard deviation to the fit templates of each process. This takes into account differences in yield and shape. The uncertainties on the e, μ, τ_h energy scale are propagated to the M_{col} and BDT distributions. For τ_h , the energy scale uncertainty is treated independently for each reconstructed hadronic decay mode of the τ lepton. The systematic uncertainties in the energy resolutions of lepton candidates have negligible effect. The energy scale of muons (electrons) misidentified as hadronically decaying tau candidates ($\mu, e \rightarrow \tau_h$ energy scale) is considered independently from true hadronic tau leptons. There is also an uncertainty in the unclustered energy scale. The unclustered energy comes from jets having $p_T < 10 \text{ GeV}$ and PF candidates

Table 3: Systematic uncertainties in the expected event yields. All uncertainties are treated as correlated between the categories, except those that have two values separated by the \oplus sign. In this case, the first value is the correlated uncertainty and the second value is the uncorrelated uncertainty for each individual category. Theoretical uncertainties on VBF Higgs boson production [85] are also applied to VH production. Uncertainties on acceptance lead to migration of events between the categories, and can be correlated or anticorrelated between categories. Ranges of uncertainties for the Higgs boson production indicate the variation in size, from negative (anticorrelated) to positive (correlated).

Systematic uncertainty	$H \rightarrow \mu\tau_h$	$H \rightarrow \mu\tau_e$	$H \rightarrow e\tau_h$	$H \rightarrow e\tau_\mu$
Muon trigger/identification/isolation	2%	2%	—	2%
Electron trigger/identification/isolation	—	2%	2%	2%
Hadronic tau lepton efficiency	5%	—	5%	—
b tagging veto	2.0–4.5%	2.0–4.5%	—	2.0–4.5%
$Z \rightarrow \mu\mu, ee$ + jets background	—	10% \oplus 5%	—	10% \oplus 5%
$Z \rightarrow \tau\tau$ + jets background	10% \oplus 5%	10% \oplus 5%	10% \oplus 5%	10% \oplus 5%
W + jets background	—	10%	—	10%
QCD multijet background	—	30%	—	30%
WW, ZZ background	5% \oplus 5%	5% \oplus 5%	5% \oplus 5%	5% \oplus 5%
$t\bar{t}$ background	10% \oplus 5%	10% \oplus 5%	10% \oplus 5%	10% \oplus 5%
$W\gamma$ background	—	10% \oplus 5%	—	10% \oplus 5%
Single top quark background	5% \oplus 5%	5% \oplus 5%	5% \oplus 5%	5% \oplus 5%
$\mu \rightarrow \tau_h$ background	25%	—	—	—
$e \rightarrow \tau_h$ background	—	—	12%	—
Jet $\rightarrow \tau_h, \mu, e$ background	30% \oplus 10%	—	30% \oplus 10%	—
Jet energy scale	3–20%	3–20%	3–20%	3–20%
τ_h energy scale	1.2%	—	1.2%	—
$\mu, e \rightarrow \tau_h$ energy scale	1.5%	—	3%	—
e energy scale	—	0.1–0.5%	0.1–0.5%	0.1–0.5%
μ energy scale	0.2%	0.2%	—	0.2%
Unclustered energy scale	$\pm 1\sigma$	$\pm 1\sigma$	$\pm 1\sigma$	$\pm 1\sigma$
Renorm./fact. scales (ggH) [85]			3.9%	
Renorm./fact. scales (VBF and VH) [85]			0.4%	
PDF + α_s (ggH) [85]			3.2%	
PDF + α_s (VBF and VH) [85]			2.1%	
Renorm./fact. acceptance (ggH)			–3.0% – +2.0%	
Renorm./fact. acceptance (VBF and VH)			–0.3% – +1.0%	
PDF + α_s acceptance (ggH)			–1.5% – +0.5%	
PDF + α_s acceptance (VBF and VH)			–1.5% – +1.0%	
Integrated luminosity			2.5%	

not within jets. It is propagated to p_T^{miss} . The unclustered energy scale is considered independently for charged particles, photons, neutral hadrons, and very forward particles which are not contained in jets. The effect of varying the energy of each particle by its uncertainty leads to changes in both shape of the distribution and yield. The four different systematic uncertainties are uncorrelated.

The uncertainties in the Higgs boson production cross sections due to the factorization and the renormalization scales, as well as the parton distribution functions (PDF) and the strong coupling constant (α_s), result in changes in normalization and they are taken from Ref. [85]. They also affect the acceptance and lead to the migration of events between the categories. They are listed as acceptance uncertainties in Table 3 and depend on the production process, Higgs boson decay channel, and category. For the ggH production this variation on the acceptance varies from -3% (anticorrelated between the categories) to 2% (correlated) for the factorization and the renormalization scales, and from -1.5% to 0.5% for PDF and α_s . For the VBF and associated production (VH) the ranges go from -0.3% to 1.0% for the factorization and the renormalization scales, and from -1.5% to 1.0% for PDF and α_s .

The bin-by-bin uncertainties account for the statistical uncertainties in every bin of the template distributions of every process. They are uncorrelated between bins, processes, and categories. The uncertainty of 2.5% on the integrated luminosity [87] affects all processes with the normalization taken directly from simulation. Shape uncertainties related to the pileup have been considered by varying the weights applied to simulation. The weight variation is obtained by a 5% change of the total inelastic cross section used to estimate the number of pileup events in data. The new values are then used to compute the weights for the simulation samples and these are applied, event by event, to produce alternate collinear mass and BDT distributions used as shape uncertainties in the fit. Other minimum bias event modelling and simulation uncertainties are estimated to be much smaller than those on the rate and are therefore neglected.

8 Results

After applying the selection criteria, a maximum likelihood fit is performed to derive the expected and observed limits. Each systematic uncertainty is used as a nuisance parameter in the fit. The fits are performed simultaneously in all channels and categories. A profile likelihood ratio is used as test statistic. The upper limits on the signal branching fraction are calculated with the asymptotic formula, using the CL_s criterion [88–90].

The BDT discriminator distributions of signal and background for each category are shown in Fig. 4 and 7 in the $H \rightarrow \mu\tau$ and $H \rightarrow e\tau$ channels respectively. Figures 5 and 8 show the corresponding M_{col} distributions used as cross-check. All the distributions are shown after they have been adjusted by the fit. No excess over the background expectation is observed. The observed and median expected 95% CL upper limits, and best fit branching fractions, for $\mathcal{B}(H \rightarrow \mu\tau)$ and $\mathcal{B}(H \rightarrow e\tau)$, assuming $m_H=125$ GeV, are given for each category in Tables 4-7. The limits are also summarized graphically in Figs. 6 and 9.

No evidence is found for either the $H \rightarrow \mu\tau$ or $H \rightarrow e\tau$ processes in this search. The observed exclusion limits are a significant improvement over the 8 TeV results. The new results exclude the branching fraction that corresponded to the best fit for the 2.4σ excess observed in the 8 TeV $H \rightarrow \mu\tau$ channel results at 95% CL, in both the M_{col} fit and BDT fit analysis. Table 8 shows a summary of the new 95% CL upper limits. The BDT fit analysis is more sensitive than the M_{col} fit analysis, with expected limits reduced by about a factor of two. In both cases the results are

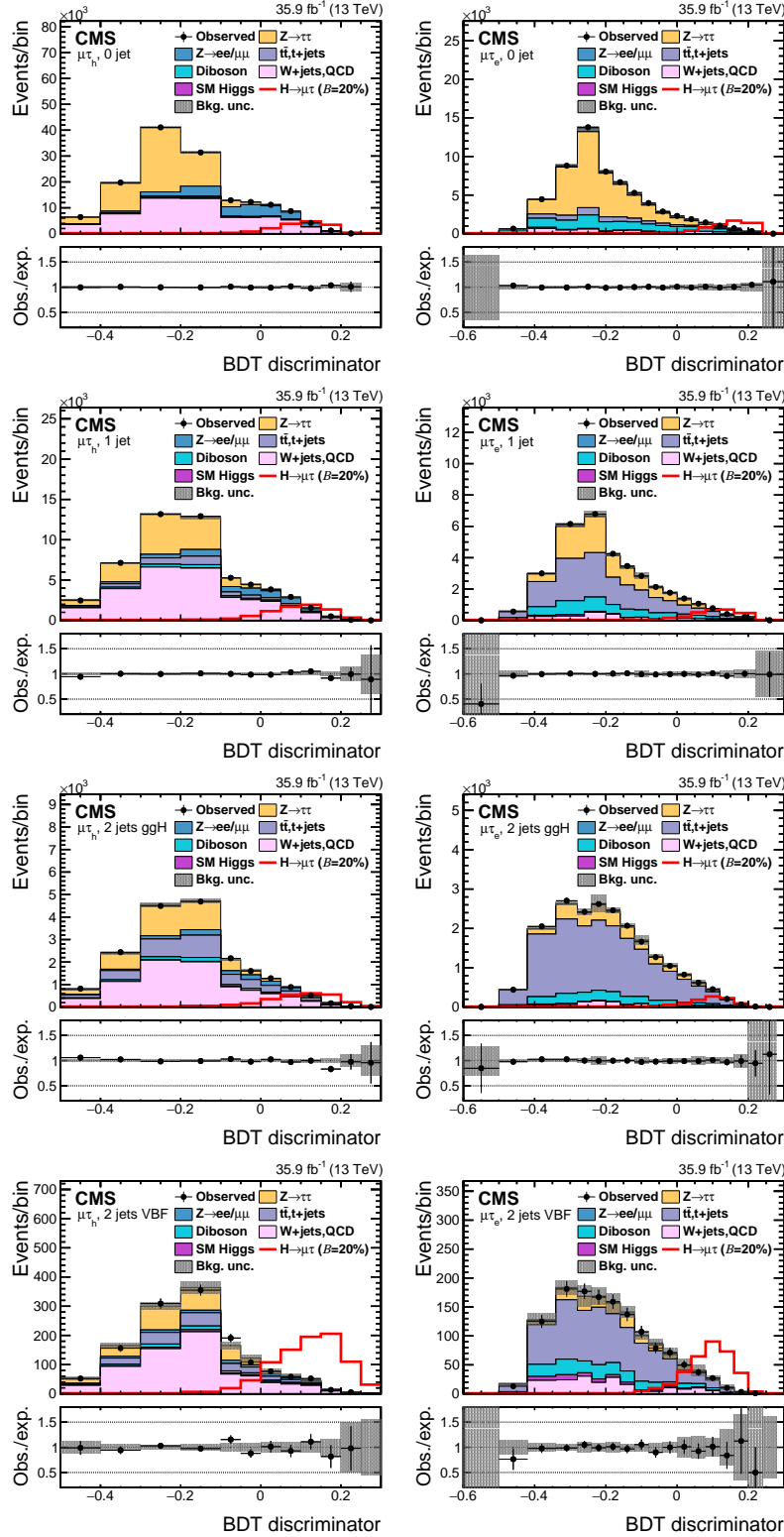


Figure 4: Distribution of the BDT discriminator for the $H \rightarrow \mu\tau$ process in the BDT fit analysis, in the individual channels and categories compared to the signal and background estimation. The background is normalized to the best fit values from the signal plus background fit while the simulated signal corresponds to $\mathcal{B}(H \rightarrow \mu\tau) = 5\%$. The bottom panel in each plot shows the fractional difference between the observed data and the fitted background. The left column of plots corresponds to the $H \rightarrow \mu\tau_h$ categories, from 0-jets (first row) to 2-jets VBF (fourth row). The right one to their $H \rightarrow \mu\tau_e$ counterparts.

Table 4: Expected and observed upper limits at 95% CL, and best fit branching fractions in percent for each individual jet category, and combined, in the $H \rightarrow \mu\tau$ process obtained with the BDT fit analysis.

Expected limits (%)					
	0-jet	1-jet	2-jets	VBF	Combined
$\mu\tau_e$	<0.83	<1.19	<1.98	<1.62	<0.59
$\mu\tau_h$	<0.43	<0.56	<0.94	<0.58	<0.29
$\mu\tau$	<0.25				
Observed limits (%)					
	0-jet	1-jet	2-jets	VBF	Combined
$\mu\tau_e$	<1.30	<1.34	<2.27	<1.79	<0.86
$\mu\tau_h$	<0.51	<0.53	<0.56	<0.51	<0.27
$\mu\tau$	<0.25				
Best fit branching fractions (%)					
	0-jet	1-jet	2-jets	VBF	Combined
$\mu\tau_e$	0.61 ± 0.36	0.22 ± 0.46	0.39 ± 0.83	0.10 ± 1.37	0.35 ± 0.26
$\mu\tau_h$	0.12 ± 0.20	-0.05 ± 0.25	-0.72 ± 0.43	-0.22 ± 0.31	-0.04 ± 0.14
$\mu\tau$	0.00 ± 0.12				

Table 5: Expected and observed upper limits at 95% CL, and best fit branching fractions in percent for each individual jet category, and combined, in the $H \rightarrow \mu\tau$ process obtained with the M_{col} fit analysis.

Expected limits (%)					
	0-jet	1-jet	2-jets	VBF	Combined
$\mu\tau_e$	<1.01	<1.47	<3.23	<1.73	<0.75
$\mu\tau_h$	<1.14	<1.26	<2.12	<1.41	<0.71
$\mu\tau$	<0.49				
Observed limits (%)					
	0-jet	1-jet	2-jets	VBF	Combined
$\mu\tau_e$	<1.08	<1.35	<3.33	<1.40	<0.71
$\mu\tau_h$	<1.04	<1.74	<1.65	<1.30	<0.66
$\mu\tau$	<0.51				
Best fit branching fractions (%)					
	0-jet	1-jet	2-jets	VBF	Combined
$\mu\tau_e$	0.13 ± 0.43	-0.22 ± 0.75	0.22 ± 1.39	-1.73 ± 1.05	-0.04 ± 0.33
$\mu\tau_h$	-0.30 ± 0.45	0.68 ± 0.56	-1.23 ± 1.04	-0.23 ± 0.66	-0.08 ± 0.34
$\mu\tau$	0.02 ± 0.20				

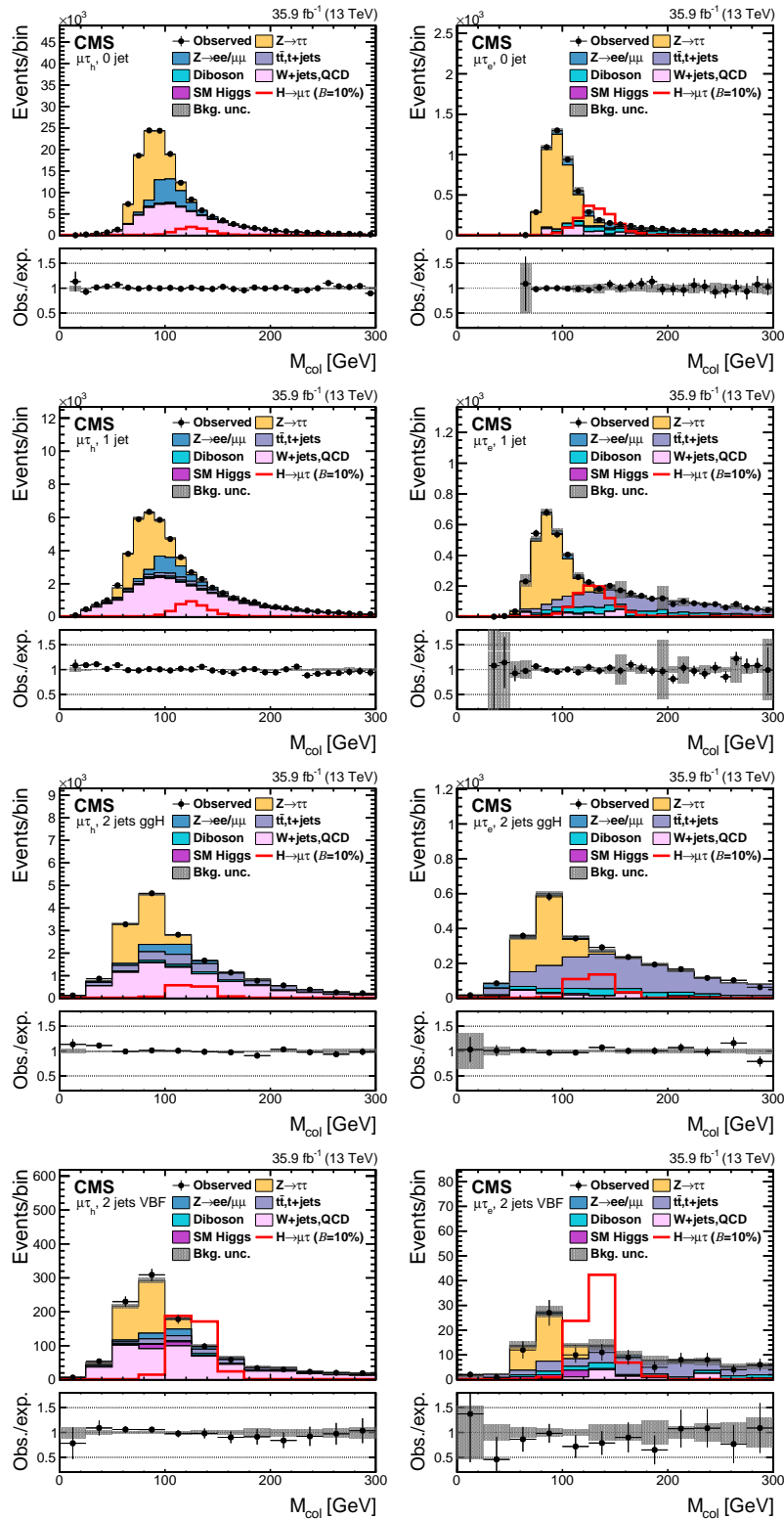


Figure 5: Distribution of the collinear mass M_{col} for the $H \rightarrow \mu\tau$ process in M_{col} fit analysis, in different channels and categories compared to the signal and background estimation. The background is normalized to the best fit values from the signal plus background fit while the overlaid simulated signal corresponds to $\mathcal{B}(H \rightarrow \mu\tau) = 5\%$. The bottom panel in each plot shows the ratio between the observed data and the fitted background. The left column of plots corresponds to the $H \rightarrow \mu\tau_h$ categories, from 0-jets (first row) to 2-jets VBF (fourth row). The right one to their $H \rightarrow \mu\tau_e$ counterparts.

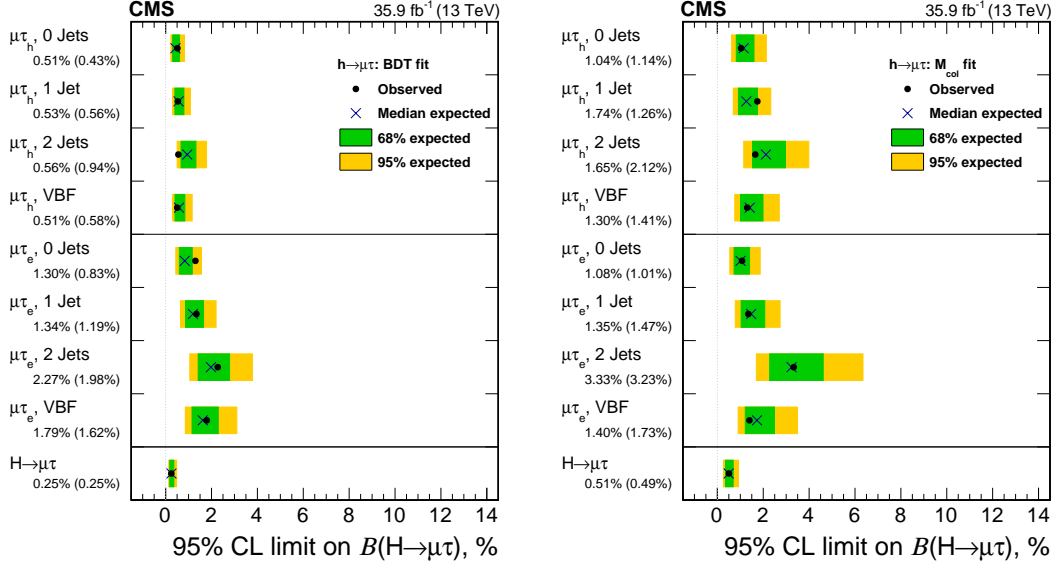


Figure 6: Observed and expected 95% CL upper limits on the $\mathcal{B}(H \rightarrow \mu\tau)$ for each individual category and combined. Left: BDT fit analysis. Right: M_{col} fit analysis.

Table 6: Expected and observed upper limits at 95% CL and best fit branching fractions in percent for each individual jet category, and combined, in the $H \rightarrow e\tau$ process obtained with the BDT fit analysis.

Expected limits (%)					
	0-jet	1-jet	2-jets	VBF	Combined
$e\tau_\mu$	<0.90	<1.59	<2.54	<1.84	<0.64
$e\tau_h$	<0.79	<1.13	<1.59	<0.74	<0.49
$e\tau$			<0.37		

Observed limits (%)					
	0-jet	1-jet	2-jets	VBF	Combined
$e\tau_\mu$	<1.22	<1.66	<2.25	<1.10	<0.78
$e\tau_h$	<0.73	<0.81	<1.94	<1.49	<0.72
$e\tau$			<0.61		

Best fit branching fractions (%)					
	0-jet	1-jet	2-jets	VBF	Combined
$e\tau_\mu$	0.47 ± 0.42	0.17 ± 0.79	-0.42 ± 1.01	-1.54 ± 0.44	0.18 ± 0.32
$e\tau_h$	-0.13 ± 0.39	-0.63 ± 0.40	0.54 ± 0.53	0.70 ± 0.38	0.33 ± 0.24
$e\tau$			0.30 ± 0.18		

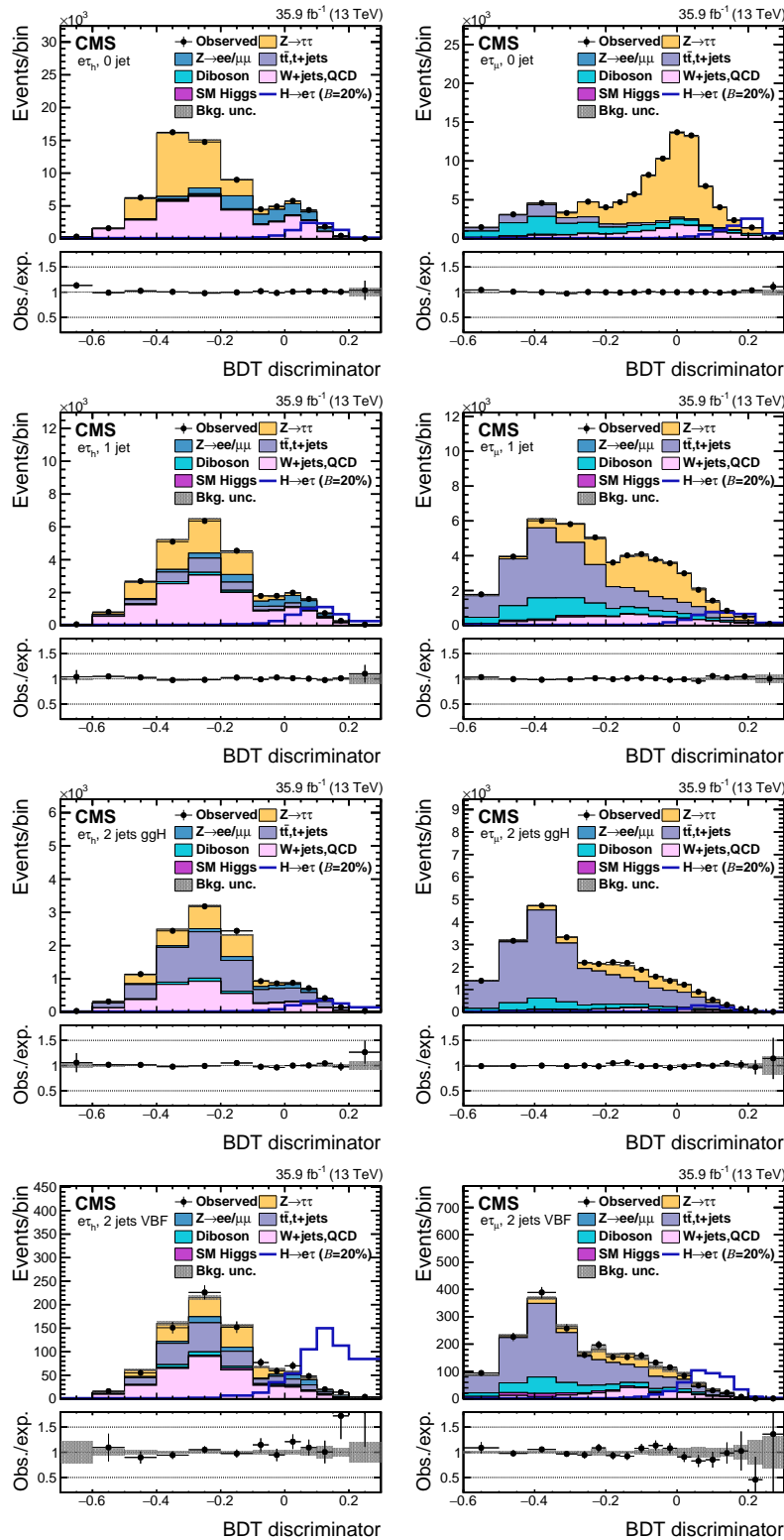


Figure 7: Distribution of the BDT discriminator for the $H \rightarrow e\tau$ process for the BDT fit analysis, in different channels and categories compared to the signal and background estimation. The background is normalized to the best fit values from the signal plus background fit while the simulated signal corresponds to $\mathcal{B}(H \rightarrow e\tau) = 5\%$. The bottom panel in each plot shows the ratio between the observed data and the fitted background. The left column of plots corresponds to the $H \rightarrow e\tau_h$ categories, from 0-jets (first row) to 2-jets VBF (fourth row). The right one to their $H \rightarrow e\tau_\mu$ counterparts.

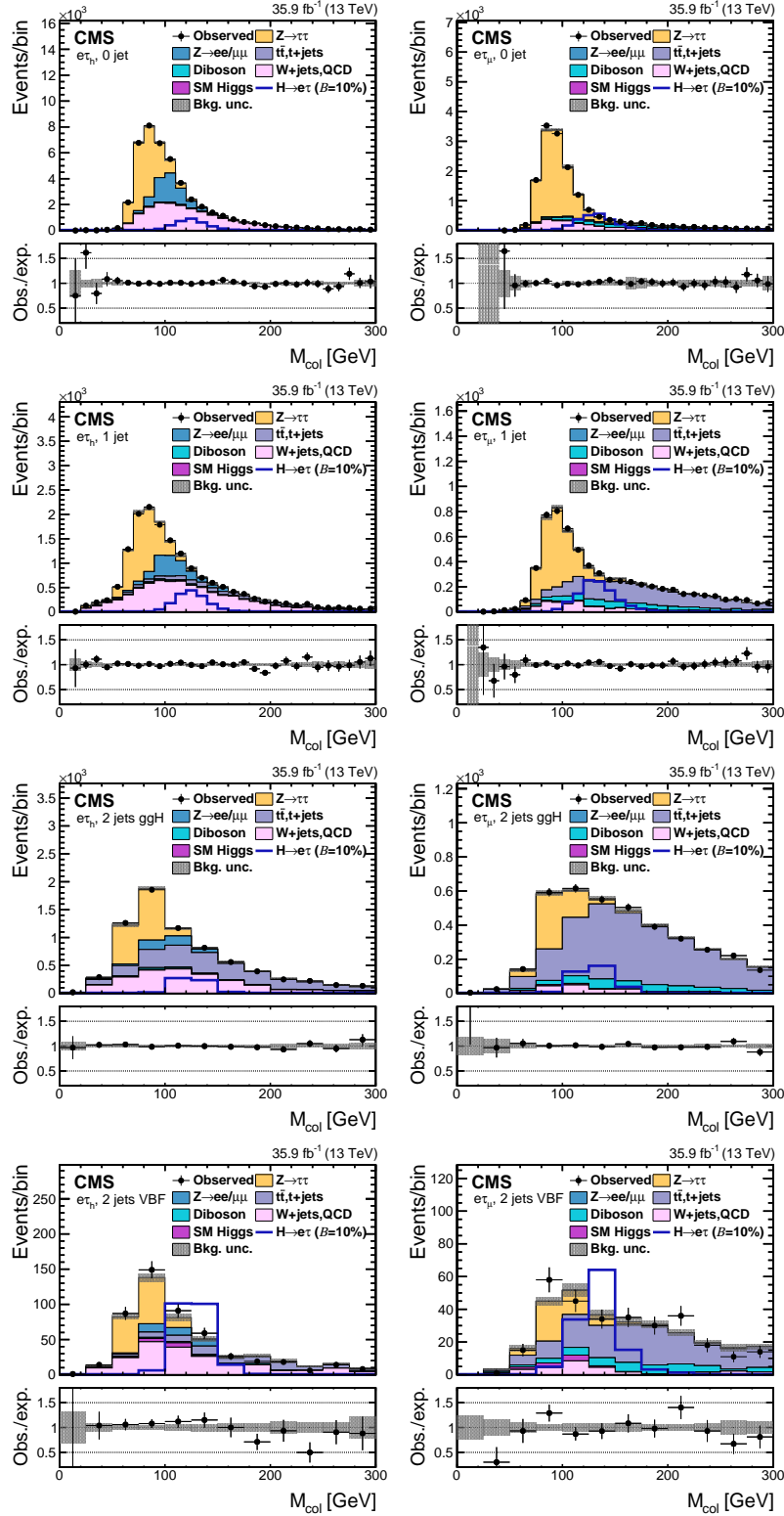


Figure 8: Distribution of the collinear mass M_{col} for the $H \rightarrow e\tau$ process in the M_{col} fit analysis, in different channels and categories compared to the signal and background estimation. The background is normalized to the best fit values from the signal plus background fit while the simulated signal corresponds to $\mathcal{B}(H \rightarrow e\tau) = 5\%$. The lower panel in each plot shows the ratio between the observed data and the fitted background. The left column of plots correspond to the $H \rightarrow e\tau_h$ categories, from 0-jets (first row) to 2 jets VBF (fourth row). The right one to their $H \rightarrow e\tau_\mu$ counterparts.

Table 7: Expected and observed upper limits at 95% CL and best fit branching fractions in percent for each individual jet category, and combined, in the $H \rightarrow e\tau$ process obtained with the M_{col} fit analysis.

Expected limits (%)					
	0-jet	1-jet	2-jets	VBF	Combined
$e\tau_\mu$	<0.94	<1.21	<3.73	<2.76	<0.71
$e\tau_h$	<1.52	<1.93	<3.55	<1.76	<0.97
$e\tau$	<0.56				

Observed limits (%)					
	0-jet	1-jet	2-jets	VBF	Combined
$e\tau_\mu$	<1.27	<1.26	<3.90	<1.78	<0.85
$e\tau_h$	<1.53	<2.07	<3.65	<3.39	<1.31
$e\tau$	<0.72				

Best fit branching fractions (%)					
	0-jet	1-jet	2-jets	VBF	Combined
$e\tau_\mu$	0.46 ± 0.43	0.07 ± 0.39	0.13 ± 1.13	-1.38 ± 1.03	0.21 ± 0.36
$e\tau_h$	0.18 ± 0.35	0.45 ± 0.60	0.29 ± 1.13	2.03 ± 0.47	0.51 ± 0.41
$e\tau$	0.23 ± 0.24				

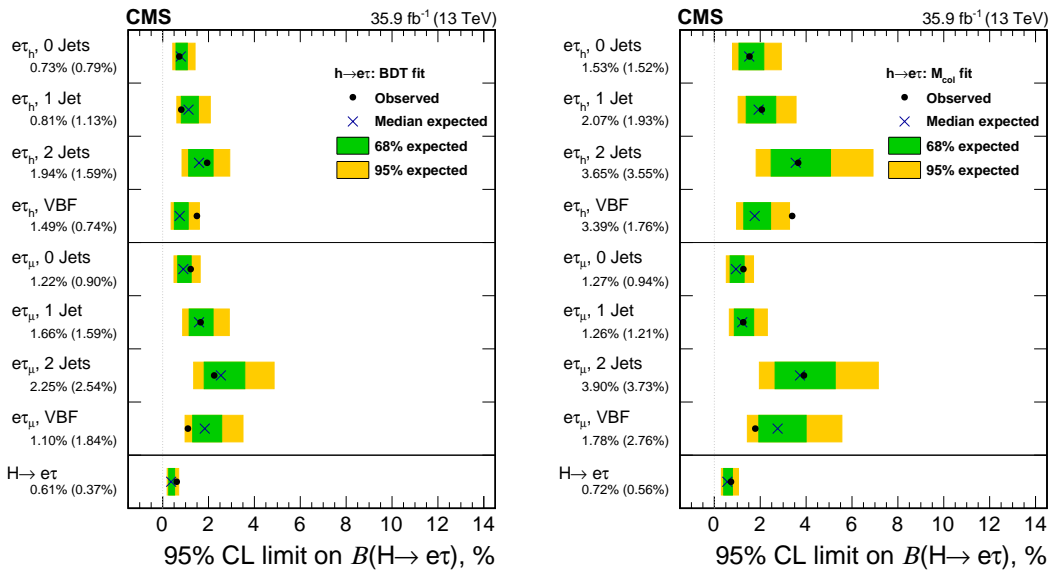


Figure 9: Observed and expected 95% CL upper limits on the $B(H \rightarrow e\tau)$ for each individual category and combined. Left: BDT fit analysis. Right: M_{col} fit analysis.

dominated by the systematic uncertainties.

Table 8: Summary of the observed and expected upper limits at the 95% CL and the best fit branching fractions in percent for the $H \rightarrow \mu\tau$ and $H \rightarrow e\tau$ processes, for the main analysis (BDT fit) and the cross check (M_{col} fit) method.

	Observed (expected) limits (%)		Best fit branching fraction (%)	
	BDT fit	M_{col} fit	BDT fit	M_{col} fit
$H \rightarrow \mu\tau$	<0.25 (0.25)%	<0.51 (0.49) %	0.00 ± 0.12 %	0.02 ± 0.20 %
$H \rightarrow e\tau$	<0.61 (0.37) %	<0.72 (0.56) %	0.30 ± 0.18 %	0.23 ± 0.24 %

The constraints on $\mathcal{B}(H \rightarrow \mu\tau)$ and $\mathcal{B}(H \rightarrow e\tau)$ can be interpreted in terms of LFV Yukawa couplings [41]. The LFV decays $e\tau$ and $\mu\tau$ arise at tree level from the assumed flavour violating Yukawa interactions, $Y_{\ell^\alpha \ell^\beta}$ where ℓ^α, ℓ^β denote the leptons, $\ell^\alpha, \ell^\beta = e, \mu, \tau$ and $\ell^\alpha \neq \ell^\beta$. The decay width $\Gamma(H \rightarrow \ell^\alpha \ell^\beta)$ in terms of the Yukawa couplings is given by:

$$\Gamma(H \rightarrow \ell^\alpha \ell^\beta) = \frac{m_H}{8\pi} (|Y_{\ell^\beta \ell^\alpha}|^2 + |Y_{\ell^\alpha \ell^\beta}|^2),$$

and the branching fraction by:

$$\mathcal{B}(H \rightarrow \ell^\alpha \ell^\beta) = \frac{\Gamma(H \rightarrow \ell^\alpha \ell^\beta)}{\Gamma(H \rightarrow \ell^\alpha \ell^\beta) + \Gamma_{\text{SM}}}.$$

The SM H decay width is assumed to be $\Gamma_{\text{SM}} = 4.1 \text{ MeV}$ [91] for $m_H = 125 \text{ GeV}$. The 95% CL upper limit on the Yukawa couplings derived from the expression for the branching fraction above is shown in Table 9. The limits on the Yukawa couplings derived from the BDT fit analysis results are shown in Fig. 10.

Table 9: 95% CL observed upper limit on the Yukawa couplings, for the main analysis (BDT fit) and the cross check (M_{col} fit) method.

	BDT fit	M_{col} fit
$\sqrt{ Y_{\mu\tau} ^2 + Y_{\tau\mu} ^2}$	$< 1.43 \times 10^{-3}$	$< 2.05 \times 10^{-3}$
$\sqrt{ Y_{e\tau} ^2 + Y_{\tau e} ^2}$	$< 2.26 \times 10^{-3}$	$< 2.45 \times 10^{-3}$

9 Summary

The search for lepton flavour violating decays of the Higgs boson in the $\mu\tau$ and $e\tau$ channels, with the 2016 data collected by the CMS detector, is presented in this paper. The data set analysed corresponds to an integrated luminosity of 35.9 fb^{-1} of proton-proton collision data recorded at $\sqrt{s} = 13 \text{ TeV}$. The results are extracted by a fit to the output of a boosted decision trees discriminator trained to distinguish the signal from backgrounds. The results are cross-checked with an alternate analysis that fits the collinear mass distribution after applying selection criteria on kinematic variables. No evidence is found for lepton flavour violating Higgs boson decays. The observed (expected) limits on the branching fraction of the Higgs boson to $\mu\tau$ and to $e\tau$ are less than 0.25% (0.25%) and 0.61% (0.37%), respectively, at 95% confidence level. These limits constitute a significant improvement over the previously obtained limits by CMS and ATLAS using 8 TeV proton-proton collision data corresponding to an integrated luminosity of about 20 fb^{-1} . Upper limits on the off-diagonal $\mu\tau$ and $e\tau$ Yukawa couplings are derived from these constraints, $\sqrt{|Y_{\mu\tau}|^2 + |Y_{\tau\mu}|^2} < 1.43 \times 10^{-3}$ and $\sqrt{|Y_{e\tau}|^2 + |Y_{\tau e}|^2} < 2.26 \times 10^{-3}$ at 95% confidence level.

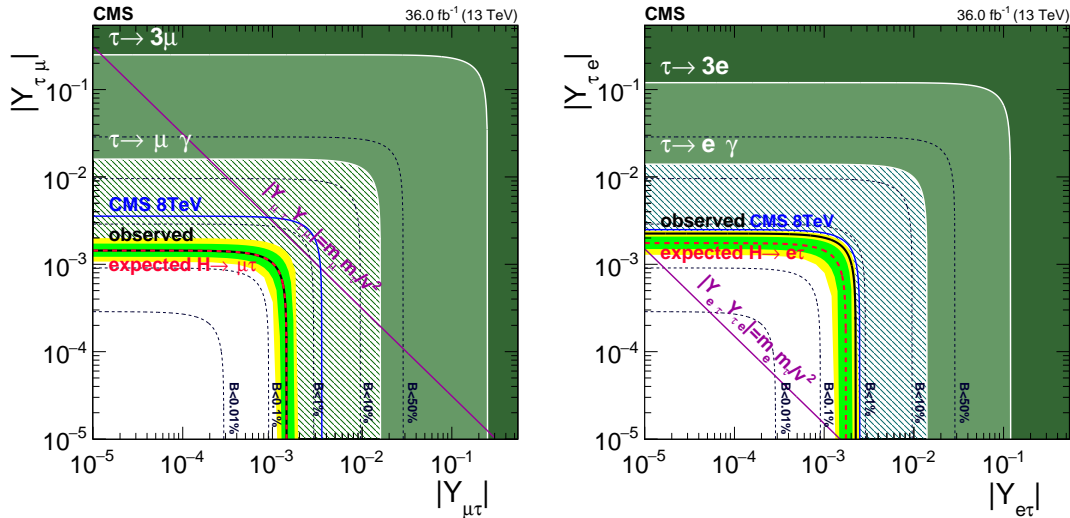


Figure 10: Constraints on the flavour violating Yukawa couplings, $|Y_{\mu\tau}|, |Y_{\tau\mu}|$ (left) and $|Y_{e\tau}|, |Y_{\tau e}|$ (right), from the BDT result. The expected (red dashed line) and observed (black solid line) limits are derived from the limit on $\mathcal{B}(H \rightarrow \mu\tau)$ and $\mathcal{B}(H \rightarrow e\tau)$ from the present analysis. The flavour-diagonal Yukawa couplings are approximated by their SM values. The green (yellow) band indicates the range that is expected to contain 68% (95%) of all observed limit excursions from the expected limit. The shaded regions are derived constraints from null searches for $\tau \rightarrow 3\mu$ or $\tau \rightarrow 3e$ (dark green) [41, 92, 93] and $\tau \rightarrow \mu\gamma$ or $\tau \rightarrow e\gamma$ (lighter green) [41, 93]. The green hashed region is derived by the CMS direct search presented in this paper. The blue solid lines are the CMS limits from [44] (left) and [45] (right). The purple diagonal line is the theoretical naturalness limit $|Y_{ij}Y_{ji}| \leq m_i m_j / v^2$ [41].

Acknowledgments

We congratulate our colleagues in the CERN accelerator departments for the excellent performance of the LHC and thank the technical and administrative staffs at CERN and at other CMS institutes for their contributions to the success of the CMS effort. In addition, we gratefully acknowledge the computing centres and personnel of the Worldwide LHC Computing Grid for delivering so effectively the computing infrastructure essential to our analyses. Finally, we acknowledge the enduring support for the construction and operation of the LHC and the CMS detector provided by the following funding agencies: BMWFW and FWF (Austria); FNRS and FWO (Belgium); CNPq, CAPES, FAPERJ, and FAPESP (Brazil); MES (Bulgaria); CERN; CAS, MoST, and NSFC (China); COLCIENCIAS (Colombia); MSES and CSF (Croatia); RPF (Cyprus); SENESCYT (Ecuador); MoER, ERC IUT, and ERDF (Estonia); Academy of Finland, MEC, and HIP (Finland); CEA and CNRS/IN2P3 (France); BMBF, DFG, and HGF (Germany); GSRT (Greece); OTKA and NIH (Hungary); DAE and DST (India); IPM (Iran); SFI (Ireland); INFN (Italy); MSIP and NRF (Republic of Korea); LAS (Lithuania); MOE and UM (Malaysia); BUAP, CINVESTAV, CONACYT, LNS, SEP, and UASLP-FAI (Mexico); MBIE (New Zealand); PAEC (Pakistan); MSHE and NSC (Poland); FCT (Portugal); JINR (Dubna); MON, RosAtom, RAS, RFBR and RAEP (Russia); MESTD (Serbia); SEIDI, CPAN, PCTI and FEDER (Spain); Swiss Funding Agencies (Switzerland); MST (Taipei); ThEPCenter, IPST, STAR, and NSTDA (Thailand); TUBITAK and TAEK (Turkey); NASU and SFFR (Ukraine); STFC (United Kingdom); DOE and NSF (USA).

Individuals have received support from the Marie-Curie programme and the European Research Council and Horizon 2020 Grant, contract No. 675440 (European Union); the Leventis Foundation; the A. P. Sloan Foundation; the Alexander von Humboldt Foundation; the Belgian

Federal Science Policy Office; the Fonds pour la Formation à la Recherche dans l'Industrie et dans l'Agriculture (FRIA-Belgium); the Agentschap voor Innovatie door Wetenschap en Technologie (IWT-Belgium); the Ministry of Education, Youth and Sports (MEYS) of the Czech Republic; the Council of Science and Industrial Research, India; the HOMING PLUS programme of the Foundation for Polish Science, cofinanced from European Union, Regional Development Fund, the Mobility Plus programme of the Ministry of Science and Higher Education, the National Science Center (Poland), contracts Harmonia 2014/14/M/ST2/00428, Opus 2014/13/B/ST2/02543, 2014/15/B/ST2/03998, and 2015/19/B/ST2/02861, Sonata-bis 2012/07/E/ST2/01406; the National Priorities Research Program by Qatar National Research Fund; the Programa Severo Ochoa del Principado de Asturias; the Thalys and Aristeia programmes cofinanced by EU-ESF and the Greek NSRF; the Rachadapisek Sompot Fund for Postdoctoral Fellowship, Chulalongkorn University and the Chulalongkorn Academic into Its 2nd Century Project Advancement Project (Thailand); the Welch Foundation, contract C-1845; and the Weston Havens Foundation (USA).

References

- [1] ATLAS Collaboration, "Observation of a new particle in the search for the Standard Model Higgs boson with the ATLAS detector at the LHC", *Phys. Lett. B* **716** (2012) 1, doi:10.1016/j.physletb.2012.08.020, arXiv:1207.7214.
- [2] CMS Collaboration, "Observation of a new boson at a mass of 125 GeV with the CMS experiment at the LHC", *Phys. Lett. B* **716** (2012) 30, doi:10.1016/j.physletb.2012.08.021, arXiv:1207.7235.
- [3] CMS Collaboration, "Observation of a new boson with mass near 125 GeV in pp collisions at $\sqrt{s} = 7$ and 8 TeV", *JHEP* **06** (2013) 081, doi:10.1007/JHEP06(2013)081, arXiv:1303.4571.
- [4] ATLAS, CMS Collaboration, "Measurements of the Higgs boson production and decay rates and constraints on its couplings from a combined ATLAS and CMS analysis of the LHC pp collision data at $\sqrt{s} = 7$ and 8 TeV", *JHEP* **08** (2016) 045, doi:10.1007/JHEP08(2016)045, arXiv:1606.02266.
- [5] J. L. Diaz-Cruz and J. J. Toscano, "Lepton flavor violating decays of Higgs bosons beyond the standard model", *Phys. Rev. D* **62** (2000) 116005, doi:10.1103/PhysRevD.62.116005, arXiv:hep-ph/9910233.
- [6] T. Han and D. Marfatia, " $h \rightarrow \mu\tau$ at hadron colliders", *Phys. Rev. Lett.* **86** (2001) 1442, doi:10.1103/PhysRevLett.86.1442, arXiv:hep-ph/0008141.
- [7] E. Arganda, A. M. Curiel, M. J. Herrero, and D. Temes, "Lepton flavor violating Higgs boson decays from massive seesaw neutrinos", *Phys. Rev. D* **71** (2005) 035011, doi:10.1103/PhysRevD.71.035011, arXiv:hep-ph/0407302.
- [8] A. Arhrib, Y. Cheng, and O. C. W. Kong, "Comprehensive analysis on lepton flavor violating Higgs boson to $\mu\bar{\tau} + \tau\bar{\mu}$ decay in supersymmetry without R parity", *Phys. Rev. D* **87** (2013) 015025, doi:10.1103/PhysRevD.87.015025, arXiv:1210.8241.
- [9] M. Arana-Catania, E. Arganda, and M. J. Herrero, "Non-decoupling SUSY in LFV Higgs decays: a window to new physics at the LHC", *JHEP* **09** (2013) 160, doi:10.1007/JHEP09(2013)160, arXiv:1304.3371. [Erratum: doi:10.1007/JHEP10(2015)192].

- [10] E. Arganda, M. J. Herrero, R. Morales, and A. Szyrkman, "Analysis of the $h, H, A \rightarrow \tau\mu$ decays induced from SUSY loops within the Mass Insertion Approximation", *JHEP* **03** (2016) 055, doi:10.1007/JHEP03(2016)055, arXiv:1510.04685.
- [11] E. Arganda, M. J. Herrero, X. Marcano, and C. Weiland, "Enhancement of the lepton flavor violating Higgs boson decay rates from SUSY loops in the inverse seesaw model", *Phys. Rev. D* **93** (2016) 055010, doi:10.1103/PhysRevD.93.055010, arXiv:1508.04623.
- [12] M. E. Gomez, S. Heinemeyer, and M. Rehman, "Lepton flavor violating higgs boson decays in supersymmetric high scale seesaw models", (2017). arXiv:1703.02229.
- [13] H.-B. Zhang et al., "125 GeV Higgs decay with lepton flavor violation in the $\mu\nu$ SSM", *Chin. Phys. C* **41** (2017) 043106, doi:10.1088/1674-1137/41/4/043106, arXiv:1511.08979.
- [14] K. Agashe and R. Contino, "Composite Higgs-mediated flavor-changing neutral current", *Phys. Rev. D* **80** (2009) 075016, doi:10.1103/PhysRevD.80.075016, arXiv:0906.1542.
- [15] A. Azatov, M. Toharia, and L. Zhu, "Higgs mediated flavor changing neutral currents in warped extra dimensions", *Phys. Rev. D* **80** (2009) 035016, doi:10.1103/PhysRevD.80.035016, arXiv:0906.1990.
- [16] G. Perez and L. Randall, "Natural neutrino masses and mixings from warped geometry", *JHEP* **01** (2009) 077, doi:10.1088/1126-6708/2009/01/077, arXiv:0805.4652.
- [17] S. Casagrande et al., "Flavor physics in the Randall-Sundrum model I. Theoretical setup and electroweak precision tests", *JHEP* **10** (2008) 094, doi:10.1088/1126-6708/2008/10/094, arXiv:0807.4937.
- [18] A. J. Buras, B. Duling, and S. Gori, "The impact of Kaluza-Klein fermions on Standard Model fermion couplings in a RS model with custodial protection", *JHEP* **09** (2009) 076, doi:10.1088/1126-6708/2009/09/076, arXiv:0905.2318.
- [19] J. D. Bjorken and S. Weinberg, "Mechanism for nonconservation of muon number", *Phys. Rev. Lett.* **38** (1977) 622, doi:10.1103/PhysRevLett.38.622.
- [20] J.-P. Lee and K. Y. Lee, " $B_s \rightarrow \mu\tau$ and $h \rightarrow \mu\tau$ decays in the general two Higgs doublet model", (2016). arXiv:1612.04057.
- [21] H. Ishimori et al., "Non-Abelian Discrete Symmetries in Particle Physics", *Prog. Theor. Phys. Suppl.* **183** (2010) 1, doi:10.1143/PTPS.183.1, arXiv:1003.3552.
- [22] M. Blanke et al., " $\Delta F = 2$ observables and fine-tuning in a warped extra dimension with custodial protection", *JHEP* **03** (2009) 001, doi:10.1088/1126-6708/2009/03/001, arXiv:0809.1073.
- [23] G. F. Giudice and O. Lebedev, "Higgs-dependent Yukawa couplings", *Phys. Lett. B* **665** (2008) 79, doi:10.1016/j.physletb.2008.05.062, arXiv:0804.1753.
- [24] J. A. Aguilar-Saavedra, "A minimal set of top-Higgs anomalous couplings", *Nucl. Phys. B* **821** (2009) 215, doi:10.1016/j.nuclphysb.2009.06.022, arXiv:0904.2387.

-
- [25] M. E. Albrecht et al., “Electroweak and flavour structure of a warped extra dimension with custodial protection”, *JHEP* **09** (2009) 064, doi:10.1088/1126-6708/2009/09/064, arXiv:0903.2415.
- [26] A. Goudelis, O. Lebedev, and J. H. Park, “Higgs-induced lepton flavor violation”, *Phys. Lett. B* **707** (2012) 369, doi:10.1016/j.physletb.2011.12.059, arXiv:1111.1715.
- [27] D. McKeen, M. Pospelov, and A. Ritz, “Modified Higgs branching ratios versus CP and lepton flavor violation”, *Phys. Rev. D* **86** (2012) 113004, doi:10.1103/PhysRevD.86.113004, arXiv:1208.4597.
- [28] A. Pilaftsis, “Lepton flavour nonconservation in H^0 decays”, *Phys. Lett. B* **285** (1992) 68, doi:10.1016/0370-2693(92)91301-O.
- [29] J. G. Körner, A. Pilaftsis, and K. Schilcher, “Leptonic CP asymmetries in flavor-changing H^0 decays”, *Phys. Rev. D* **47** (1993) 1080, doi:10.1103/PhysRevD.47.1080.
- [30] E. Arganda, M. J. Herrero, X. Marcano, and C. Weiland, “Imprints of massive inverse seesaw model neutrinos in lepton flavor violating Higgs boson decays”, *Phys. Rev. D* **91** (2015) 015001, doi:10.1103/PhysRevD.91.015001, arXiv:1405.4300.
- [31] J. Herrero-Garcia, N. Rius, and A. Santamaria, “Higgs lepton flavour violation: UV completions and connection to neutrino masses”, *JHEP* **11** (2016) 084, doi:10.1007/JHEP11(2016)084, arXiv:1605.06091.
- [32] F. del Aguila et al., “Lepton flavor changing higgs decays in the littlest Higgs model with T-parity”, *JHEP* **08** (2017) 028, doi:10.1007/JHEP08(2017)028, arXiv:1705.08827.
- [33] N. H. Thao, L. T. Hue, H. T. Hung, and N. T. Xuan, “Lepton flavor violating Higgs boson decays in seesaw models: New discussions”, *Nucl. Phys. B* **921** (2017) 159, doi:10.1016/j.nuclphysb.2017.05.014, arXiv:1703.00896.
- [34] I. Galon and J. Zupan, “Dark sectors and enhanced $h \rightarrow \tau\mu$ transitions”, *JHEP* **05** (2017) 083, doi:10.1007/JHEP05(2017)083, arXiv:1701.08767.
- [35] E. Arganda et al., “Effective lepton flavor violating $H\ell_i\ell_j$ vertex from right-handed neutrinos within the mass insertion approximation”, *Phys. Rev. D* **95** (2017) 095029, doi:10.1103/PhysRevD.95.095029, arXiv:1612.09290.
- [36] D. Choudhury, A. Kundu, S. Nandi, and S. K. Patra, “Unified resolution of the $R(D)$ and $R(D^*)$ anomalies and the lepton flavor violating decay $h \rightarrow \mu\tau$ ”, *Phys. Rev. D* **95** (2017) 035021, doi:10.1103/PhysRevD.95.035021, arXiv:1612.03517.
- [37] B. McWilliams and L.-F. Li, “Virtual effects of Higgs particles”, *Nucl. Phys. B* **179** (1981) 62, doi:10.1016/0550-3213(81)90249-2.
- [38] O. U. Shanker, “Flavour violation, scalar particles and leptoquarks”, *Nucl. Phys. B* **206** (1982) 253, doi:10.1016/0550-3213(82)90534-X.
- [39] A. Celis, V. Cirigliano, and E. Passemar, “Lepton flavor violation in the Higgs sector and the role of hadronic tau-lepton decays”, *Phys. Rev. D* **89** (2014) 013008, doi:10.1103/PhysRevD.89.013008, arXiv:1309.3564.

- [40] G. Blankenburg, J. Ellis, and G. Isidori, “Flavour-changing decays of a 125 GeV Higgs-like particle”, *Phys. Lett. B* **712** (2012) 386, doi:10.1016/j.physletb.2012.05.007, arXiv:1202.5704.
- [41] R. Harnik, J. Kopp, and J. Zupan, “Flavor violating higgs decays”, *JHEP* **03** (2013) 26, doi:10.1007/JHEP03(2013)026, arXiv:1209.1397.
- [42] S. M. Barr and A. Zee, “Electric dipole moment of the electron and of the neutron”, *Phys. Rev. Lett.* **65** (1990) 21, doi:10.1103/PhysRevLett.65.21.
- [43] MEG Collaboration, “Search for the lepton flavour violating decay $\mu^+ \rightarrow e^+ \gamma$ with the full dataset of the MEG experiment”, *Eur. Phys. J. C* **76** (2016) 434, doi:10.1140/epjc/s10052-016-4271-x, arXiv:1605.05081.
- [44] CMS Collaboration, “Search for lepton-flavour-violating decays of the Higgs boson”, *Phys. Lett. B* **749** (2015) 337, doi:10.1016/j.physletb.2015.07.053, arXiv:1502.07400.
- [45] CMS Collaboration, “Search for lepton flavour violating decays of the higgs boson to $e\tau$ and $e\mu$ in proton-proton collisions at $\sqrt{s} = 8$ TeV”, *Phys. Lett. B* **763** (2016) 472, doi:10.1016/j.physletb.2016.09.062, arXiv:1607.03561.
- [46] ATLAS Collaboration, “Search for lepton-flavour-violating decays of the Higgs and Z bosons with the ATLAS detector”, *Eur. Phys. J. C* **77** (2017) 70, doi:10.1140/epjc/s10052-017-4624-0, arXiv:1604.07730.
- [47] ATLAS Collaboration, “Search for lepton-flavour-violating $H \rightarrow \mu\tau$ decays of the Higgs boson with the ATLAS detector”, *JHEP* **11** (2015) 211, doi:10.1007/JHEP11(2015)211, arXiv:1508.03372.
- [48] CMS Collaboration, “Evidence for the direct decay of the 125 GeV Higgs boson to fermions”, *Nature Phys.* **10** (2014) 557, doi:10.1038/nphys3005, arXiv:1401.6527.
- [49] CMS Collaboration, “Evidence for the 125 GeV Higgs boson decaying to a pair of τ leptons”, *JHEP* **05** (2014) 104, doi:10.1007/JHEP05(2014)104, arXiv:1401.5041.
- [50] CMS Collaboration, “Observation of the Higgs boson decay to a pair of τ leptons”, (2017). arXiv:1708.00373. Submitted to *Phys. Lett. B*.
- [51] ATLAS Collaboration, “Evidence for the Higgs-boson Yukawa coupling to tau leptons with the ATLAS detector”, *JHEP* **04** (2015) 117, doi:10.1007/JHEP04(2015)117, arXiv:1501.04943.
- [52] CMS Collaboration, “The CMS trigger system”, *J. Instrum.* **12** (2017) P01020, doi:10.1088/1748-0221/12/01/P01020, arXiv:1609.02366.
- [53] CMS Collaboration, “The CMS experiment at the CERN LHC”, *JINST* **3** (2008) S08004, doi:10.1088/1748-0221/3/08/S08004.
- [54] H. M. Georgi, S. L. Glashow, M. E. Machacek, and D. V. Nanopoulos, “Higgs bosons from two gluon annihilation in proton proton collisions”, *Phys. Rev. Lett.* **40** (1978) 692, doi:10.1103/PhysRevLett.40.692.
- [55] R. N. Cahn, S. D. Ellis, R. Kleiss, and W. J. Stirling, “Transverse-momentum signatures for heavy Higgs bosons”, *Phys. Rev. D* **35** (1987) 1626, doi:10.1103/PhysRevD.35.1626.

-
- [56] S. L. Glashow, D. V. Nanopoulos, and A. Yildiz, “Associated production of Higgs bosons and Z particles”, *Phys. Rev. D* **18** (1978) 1724, doi:10.1103/PhysRevD.18.1724.
- [57] P. Nason, “A new method for combining NLO QCD with shower Monte Carlo algorithms”, *JHEP* **11** (2004) 040, doi:10.1088/1126-6708/2004/11/040, arXiv:hep-ph/0409146.
- [58] S. Frixione, P. Nason, and C. Oleari, “Matching NLO QCD computations with parton shower simulations: the POWHEG method”, *JHEP* **11** (2007) 070, doi:10.1088/1126-6708/2007/11/070, arXiv:0709.2092.
- [59] S. Alioli, P. Nason, C. Oleari, and E. Re, “A general framework for implementing NLO calculations in shower Monte Carlo programs: the POWHEG BOX”, *JHEP* **06** (2010) 043, doi:10.1007/JHEP06(2010)043, arXiv:1002.2581.
- [60] S. Alioli et al., “Jet pair production in POWHEG”, *JHEP* **04** (2011) 081, doi:10.1007/JHEP04(2011)081, arXiv:1012.3380.
- [61] S. Alioli, P. Nason, C. Oleari, and E. Re, “NLO Higgs boson production via gluon fusion matched with shower in POWHEG”, *JHEP* **04** (2009) 002, doi:10.1088/1126-6708/2009/04/002, arXiv:0812.0578.
- [62] E. Bagnaschi, G. Degrossi, P. Slavich, and A. Vicini, “Higgs production via gluon fusion in the POWHEG approach in the SM and in the MSSM”, *JHEP* **02** (2012) 088, doi:10.1007/JHEP02(2012)088, arXiv:1111.2854.
- [63] G. Luisoni, P. Nason, C. Oleari, and F. Tramontano, “ $HW^\pm/HZ + 0$ and 1 jet at NLO with the POWHEG BOX interfaced to GoSam and their merging within MiNLO”, *JHEP* **10** (2013) 083, doi:10.1007/JHEP10(2013)083, arXiv:1306.2542.
- [64] J. Alwall et al., “The automated computation of tree-level and next-to-leading order differential cross sections, and their matching to parton shower simulations”, *JHEP* **07** (2014) 079, doi:10.1007/JHEP07(2014)079, arXiv:1405.0301.
- [65] J. Alwall et al., “Comparative study of various algorithms for the merging of parton showers and matrix elements in hadronic collisions”, *Eur. Phys. J. C* **53** (2008) 473, doi:10.1140/epjc/s10052-007-0490-5, arXiv:0706.2569.
- [66] R. Frederix and S. Frixione, “Merging meets matching in MC@NLO”, *JHEP* **12** (2012) 061, doi:10.1007/JHEP12(2012)061, arXiv:1209.6215.
- [67] T. Sjöstrand et al., “An introduction to PYTHIA 8.2”, *Comput. Phys. Commun.* **191** (2015) 159, doi:10.1016/j.cpc.2015.01.024, arXiv:1410.3012.
- [68] CMS Collaboration, “Event generator tunes obtained from underlying event and multiparton scattering measurements”, *Eur. Phys. J. C* **76** (2016) 155, doi:10.1140/epjc/s10052-016-3988-x, arXiv:1512.00815.
- [69] GEANT4 Collaboration, “GEANT4 — a simulation toolkit”, *Nucl. Instrum. Meth. A* **506** (2003) 250, doi:10.1016/S0168-9002(03)01368-8.
- [70] CMS Collaboration, “Particle-flow reconstruction and global event description with the CMS detector”, *JINST* **12** (2017) P10003, doi:10.1088/1748-0221/12/10/P10003, arXiv:1706.04965.

- [71] M. Cacciari, G. P. Salam, and G. Soyez, "The anti- k_t jet clustering algorithm", *JHEP* **04** (2008) 063, doi:10.1088/1126-6708/2008/04/063, arXiv:0802.1189.
- [72] M. Cacciari, G. P. Salam, and G. Soyez, "FastJet user manual", *Eur. Phys. J. C* **72** (2012) 1896, doi:10.1140/epjc/s10052-012-1896-2, arXiv:1111.6097.
- [73] CMS Collaboration, "Performance of CMS muon reconstruction in pp collision events at $\sqrt{s} = 7$ TeV", *JINST* **7** (2012) P10002, doi:10.1088/1748-0221/7/10/P10002, arXiv:1206.4071.
- [74] CMS Collaboration, "Performance of electron reconstruction and selection with the CMS detector in proton-proton collisions at $\sqrt{s} = 8$ TeV", *JINST* **10** (2015) P06005, doi:10.1088/1748-0221/10/06/P06005, arXiv:1502.02701.
- [75] CMS Collaboration, "Reconstruction and identification of tau lepton decays to hadrons and ν_τ at CMS", *JINST* **11** (2016) P01019, doi:10.1088/1748-0221/11/01/P01019, arXiv:1510.07488.
- [76] CMS Collaboration, "Performance of reconstruction and identification of tau leptons in their decays to hadrons and tau neutrino in LHC Run-2", CMS Physics Analysis Summary CMS-PAS-TAU-16-002, 2016.
- [77] M. Cacciari, G. P. Salam, "Dispelling the N^3 myth for the k_t jet-finder", *Phys. Lett. B* **641** (2006) 57, doi:10.1016/j.physletb.2006.08.037, arXiv:hep-ph/0512210.
- [78] CMS Collaboration, "Determination of jet energy calibration and transverse momentum resolution in CMS", *JINST* **6** (2011) 11002, doi:10.1088/1748-0221/6/11/P11002, arXiv:1107.4277.
- [79] CMS Collaboration, "Jet energy scale and resolution in the CMS experiment in pp collisions at 8 TeV", *JINST* **12** (2017) P02014, doi:10.1088/1748-0221/12/02/P02014, arXiv:1607.03663.
- [80] M. Cacciari, G. P. Salam, and G. Soyez, "The catchment area of jets", *JHEP* **04** (2008) 005, doi:10.1088/1126-6708/2008/04/005, arXiv:0802.1188.
- [81] M. Cacciari and G. P. Salam, "Pileup subtraction using jet areas", *Phys. Lett. B* **659** (2008) 119, doi:10.1016/j.physletb.2007.09.077, arXiv:0707.1378.
- [82] CMS Collaboration, "Performance of the CMS missing transverse momentum reconstruction in pp data at $\sqrt{s} = 8$ TeV", *JINST* **10** (2015) P02006, doi:10.1088/1748-0221/10/02/P02006, arXiv:1411.0511.
- [83] R. K. Ellis, I. Hinchliffe, M. Soldate, and J. J. van der Bij, "Higgs decay to $\tau^+\tau^-$: A possible signature of intermediate mass Higgs bosons at high energy hadron colliders", *Nucl. Phys. B* **297** (1988) 221, doi:10.1016/0550-3213(88)90019-3.
- [84] CMS Collaboration, "Identification of b quark jets at the CMS Experiment in the LHC Run 2", CMS Physics Analysis Summary CMS-PAS-BTV-15-001, 2016.
- [85] D. de Florian et al., "Handbook of LHC Higgs cross sections: 4. deciphering the nature of the Higgs sector", CERN Report CERN-2017-002-M, 2016. doi:10.23731/CYRM-2017-002, arXiv:1610.07922.

- [86] CMS Collaboration, “Measurements of inclusive W and Z cross sections in pp collisions at $\sqrt{s} = 7$ TeV”, *J. High Energy Phys.* **01** (2011) 080, doi:10.1007/JHEP01(2011)080, arXiv:1012.2466.
- [87] CMS Collaboration, “CMS luminosity measurements for the 2016 data taking period”, CMS Physics Analysis Summary CMS-PAS-LUM-17-001, 2017.
- [88] T. Junk, “Confidence level computation for combining searches with small statistics”, *Nucl. Instrum. Meth. A* **434** (1999) 435, doi:10.1016/S0168-9002(99)00498-2, arXiv:hep-ex/9902006.
- [89] A. L. Read, “Presentation of search results: the CL_s technique”, in *Durham IPPP Workshop: Advanced Statistical Techniques in Particle Physics*, p. 2693. Durham, UK, March, 2002. [*J. Phys. G* **28** (2002) 2693]. doi:10.1088/0954-3899/28/10/313.
- [90] G. Cowan, K. Cranmer, E. Gross, and O. Vitells, “Asymptotic formulae for likelihood-based tests of new physics”, *Eur. Phys. J. C* **71** (2011) 1554, doi:10.1140/epjc/s10052-011-1554-0, arXiv:1007.1727. [Erratum: doi:10.1140/epjc/s10052-013-2501-z].
- [91] A. Denner et al., “Standard model Higgs-boson branching ratios with uncertainties”, *Eur. Phys. J. C* **71** (2011) 1753, doi:10.1140/epjc/s10052-011-1753-8, arXiv:1107.5909.
- [92] Belle Collaboration, “Search for lepton flavor violating τ decays into three leptons with 719 million produced $\tau^+\tau^-$ pairs”, *Phys. Lett. B* **687** (2010) 139, doi:10.1016/j.physletb.2010.03.037, arXiv:1001.3221.
- [93] Particle Data Group, C. Patrignani et al., “Review of Particle Physics”, *Chin. Phys. C* **40** (2016) 100001, doi:10.1088/1674-1137/40/10/100001.

A The CMS Collaboration

Yerevan Physics Institute, Yerevan, Armenia

A.M. Sirunyan, A. Tumasyan

Institut für Hochenergiephysik, Wien, Austria

W. Adam, F. Ambrogio, E. Asilar, T. Bergauer, J. Brandstetter, E. Brondolin, M. Dragicevic, J. Erö, M. Flechl, M. Friedl, R. Frühwirth¹, V.M. Ghete, J. Grossmann, J. Hrubec, M. Jeitler¹, A. König, N. Krammer, I. Krätschmer, D. Liko, T. Madlener, I. Mikulec, E. Pree, N. Rad, H. Rohringer, J. Schieck¹, R. Schöfbeck, M. Spanring, D. Spitzbart, W. Waltenberger, J. Wittmann, C.-E. Wulz¹, M. Zarucki

Institute for Nuclear Problems, Minsk, Belarus

V. Chekhovsky, V. Mossolov, J. Suarez Gonzalez

Universiteit Antwerpen, Antwerpen, Belgium

E.A. De Wolf, D. Di Croce, X. Janssen, J. Lauwers, M. Van De Klundert, H. Van Haeuvermaet, P. Van Mechelen, N. Van Remortel

Vrije Universiteit Brussel, Brussel, Belgium

S. Abu Zeid, F. Blekman, J. D'Hondt, I. De Bruyn, J. De Clercq, K. Deroover, G. Flouris, D. Lontkovskyi, S. Lowette, S. Moortgat, L. Moreels, Q. Python, K. Skovpen, S. Tavernier, W. Van Doninck, P. Van Mulders, I. Van Parijs

Université Libre de Bruxelles, Bruxelles, Belgium

D. Beghin, H. Brun, B. Clerbaux, G. De Lentdecker, H. Delannoy, B. Dorney, G. Fasanella, L. Favart, R. Goldouzian, A. Grebenyuk, G. Karapostoli, T. Lenzi, J. Luetic, T. Maerschalk, A. Marinov, A. Randle-conde, T. Seva, E. Starling, C. Vander Velde, P. Vanlaer, D. Vannerom, R. Yonamine, F. Zenoni, F. Zhang²

Ghent University, Ghent, Belgium

A. Cimmino, T. Cornelis, D. Dobur, A. Fagot, M. Gul, I. Khvastunov³, D. Poyraz, C. Roskas, S. Salva, M. Tytgat, W. Verbeke, N. Zaganidis

Université Catholique de Louvain, Louvain-la-Neuve, Belgium

H. Bakhshiansohi, O. Bondu, S. Brochet, G. Bruno, C. Caputo, A. Caudron, P. David, S. De Visscher, C. Delaere, M. Delcourt, B. Francois, A. Giammanco, M. Komm, G. Krintiras, V. Lemaître, A. Magitteri, A. Mertens, M. Musich, K. Piotrkowski, L. Quertenmont, A. Saggio, M. Vidal Marono, S. Wertz, J. Zobec

Université de Mons, Mons, Belgium

N. Bely

Centro Brasileiro de Pesquisas Físicas, Rio de Janeiro, Brazil

W.L. Aldá Júnior, F.L. Alves, G.A. Alves, L. Brito, M. Correa Martins Junior, C. Hensel, A. Moraes, M.E. Pol, P. Rebello Teles

Universidade do Estado do Rio de Janeiro, Rio de Janeiro, Brazil

E. Belchior Batista Das Chagas, W. Carvalho, J. Chinellato⁴, E. Coelho, E.M. Da Costa, G.G. Da Silveira⁵, D. De Jesus Damiao, S. Fonseca De Souza, L.M. Huertas Guativa, H. Malbouisson, M. Melo De Almeida, C. Mora Herrera, L. Mundim, H. Nogima, L.J. Sanchez Rosas, A. Santoro, A. Sznajder, M. Thiel, E.J. Tonelli Manganote⁴, F. Torres Da Silva De Araujo, A. Vilela Pereira

Universidade Estadual Paulista ^a, Universidade Federal do ABC ^b, São Paulo, Brazil

S. Ahuja^a, C.A. Bernardes^a, T.R. Fernandez Perez Tomei^a, E.M. Gregores^b, P.G. Mercadante^b, S.F. Novaes^a, Sandra S. Padula^a, D. Romero Abad^b, J.C. Ruiz Vargas^a

Institute for Nuclear Research and Nuclear Energy, Bulgarian Academy of Sciences, Sofia, Bulgaria

A. Aleksandrov, R. Hadjiiska, P. Iaydjiev, M. Misheva, M. Rodozov, M. Shopova, G. Sultanov

University of Sofia, Sofia, Bulgaria

A. Dimitrov, I. Glushkov, L. Litov, B. Pavlov, P. Petkov

Beihang University, Beijing, China

W. Fang⁶, X. Gao⁶, L. Yuan

Institute of High Energy Physics, Beijing, China

M. Ahmad, J.G. Bian, G.M. Chen, H.S. Chen, M. Chen, Y. Chen, C.H. Jiang, D. Leggat, H. Liao, Z. Liu, F. Romeo, S.M. Shaheen, A. Spiezia, J. Tao, C. Wang, Z. Wang, E. Yazgan, H. Zhang, S. Zhang, J. Zhao

State Key Laboratory of Nuclear Physics and Technology, Peking University, Beijing, China

Y. Ban, G. Chen, Q. Li, S. Liu, Y. Mao, S.J. Qian, D. Wang, Z. Xu

Universidad de Los Andes, Bogota, Colombia

C. Avila, A. Cabrera, C.A. Carrillo Montoya, L.F. Chaparro Sierra, C. Florez, C.F. González Hernández, J.D. Ruiz Alvarez

University of Split, Faculty of Electrical Engineering, Mechanical Engineering and Naval Architecture, Split, Croatia

B. Courbon, N. Godinovic, D. Lelas, I. Puljak, P.M. Ribeiro Cipriano, T. Sculac

University of Split, Faculty of Science, Split, Croatia

Z. Antunovic, M. Kovac

Institute Rudjer Boskovic, Zagreb, Croatia

V. Brigljevic, D. Ferencek, K. Kadija, B. Mesic, A. Starodumov⁷, T. Susa

University of Cyprus, Nicosia, Cyprus

M.W. Ather, A. Attikis, G. Mavromanolakis, J. Mousa, C. Nicolaou, F. Ptochos, P.A. Razis, H. Rykaczewski

Charles University, Prague, Czech Republic

M. Finger⁸, M. Finger Jr.⁸

Universidad San Francisco de Quito, Quito, Ecuador

E. Carrera Jarrin

Academy of Scientific Research and Technology of the Arab Republic of Egypt, Egyptian Network of High Energy Physics, Cairo, Egypt

Y. Assran^{9,10}, M.A. Mahmoud^{11,10}, A. Mahrous¹²

National Institute of Chemical Physics and Biophysics, Tallinn, Estonia

R.K. Dewanjee, M. Kadastik, L. Perrini, M. Raidal, A. Tiko, C. Veelken

Department of Physics, University of Helsinki, Helsinki, Finland

P. Eerola, H. Kirschenmann, J. Pekkanen, M. Voutilainen

Helsinki Institute of Physics, Helsinki, Finland

J. Havukainen, J.K. Heikkilä, T. Järvinen, V. Karimäki, R. Kinnunen, T. Lampén, K. Lassila-Perini, S. Laurila, S. Lehti, T. Lindén, P. Luukka, H. Siikonen, E. Tuominen, J. Tuominiemi

Lappeenranta University of Technology, Lappeenranta, Finland

J. Talvitie, T. Tuuva

IRFU, CEA, Université Paris-Saclay, Gif-sur-Yvette, France

M. Besancon, F. Couderc, M. Dejardin, D. Denegri, J.L. Faure, F. Ferri, S. Ganjour, S. Ghosh, A. Givernaud, P. Gras, G. Hamel de Monchenault, P. Jarry, I. Kucher, C. Leloup, E. Locci, M. Machet, J. Malcles, G. Negro, J. Rander, A. Rosowsky, M.Ö. Sahin, M. Titov

Laboratoire Leprince-Ringuet, Ecole polytechnique, CNRS/IN2P3, Université Paris-Saclay, Palaiseau, France

A. Abdulsalam, C. Amendola, I. Antropov, S. Baffioni, F. Beaudette, P. Busson, L. Cadamuro, C. Charlot, R. Granier de Cassagnac, M. Jo, S. Lisniak, A. Lobanov, J. Martin Blanco, M. Nguyen, C. Ochando, G. Ortona, P. Paganini, P. Pigard, R. Salerno, J.B. Sauvan, Y. Sirois, A.G. Stahl Leitner, T. Strebler, Y. Yilmaz, A. Zabi, A. Zghiche

Université de Strasbourg, CNRS, IPHC UMR 7178, F-67000 Strasbourg, France

J.-L. Agram¹³, J. Andrea, D. Bloch, J.-M. Brom, M. Buttignol, E.C. Chabert, N. Chanon, C. Collard, E. Conte¹³, X. Coubez, J.-C. Fontaine¹³, D. Gelé, U. Goerlach, M. Jansová, A.-C. Le Bihan, N. Tonon, P. Van Hove

Centre de Calcul de l'Institut National de Physique Nucleaire et de Physique des Particules, CNRS/IN2P3, Villeurbanne, France

S. Gadrat

Université de Lyon, Université Claude Bernard Lyon 1, CNRS-IN2P3, Institut de Physique Nucléaire de Lyon, Villeurbanne, France

S. Beauceron, C. Bernet, G. Boudoul, R. Chierici, D. Contardo, P. Depasse, H. El Mamouni, J. Fay, L. Finco, S. Gascon, M. Gouzevitch, G. Grenier, B. Ille, F. Lagarde, I.B. Laktineh, M. Lethuillier, L. Mirabito, A.L. Pequegnot, S. Perries, A. Popov¹⁴, V. Sordini, M. Vander Donckt, S. Viret

Georgian Technical University, Tbilisi, Georgia

A. Khvedelidze⁸

Tbilisi State University, Tbilisi, Georgia

Z. Tsamalaidze⁸

RWTH Aachen University, I. Physikalisches Institut, Aachen, Germany

C. Autermann, L. Feld, M.K. Kiesel, K. Klein, M. Lipinski, M. Preuten, C. Schomakers, J. Schulz, V. Zhukov¹⁴

RWTH Aachen University, III. Physikalisches Institut A, Aachen, Germany

A. Albert, E. Dietz-Laursonn, D. Duchardt, M. Endres, M. Erdmann, S. Erdweg, T. Esch, R. Fischer, A. Güth, M. Hamer, T. Hebbeker, C. Heidemann, K. Hoepfner, S. Knutzen, M. Merschmeyer, A. Meyer, P. Millet, S. Mukherjee, T. Pook, M. Radziej, H. Reithler, M. Rieger, F. Scheuch, D. Teyssier, S. Thüer

RWTH Aachen University, III. Physikalisches Institut B, Aachen, Germany

G. Flügge, B. Kargoll, T. Kress, A. Künsken, T. Müller, A. Nehr Korn, A. Nowack, C. Pistone, O. Pooth, A. Stahl¹⁵

Deutsches Elektronen-Synchrotron, Hamburg, Germany

M. Aldaya Martin, T. Arndt, C. Asawatangtrakuldee, K. Beernaert, O. Behnke, U. Behrens, A. Bermúdez Martínez, A.A. Bin Anuar, K. Borras¹⁶, V. Botta, A. Campbell, P. Connor, C. Contreras-Campana, F. Costanza, C. Diez Pardos, G. Eckerlin, D. Eckstein, T. Eichhorn, E. Eren, E. Gallo¹⁷, J. Garay Garcia, A. Geiser, A. Gzhko, J.M. Grados Luyando, A. Grohsjean, P. Gunnellini, M. Guthoff, A. Harb, J. Hauk, M. Hempel¹⁸, H. Jung, A. Kalogeropoulos, M. Kasemann, J. Keaveney, C. Kleinwort, I. Korol, D. Krücker, W. Lange, A. Lelek, T. Lenz, J. Leonard, K. Lipka, W. Lohmann¹⁸, R. Mankel, I.-A. Melzer-Pellmann, A.B. Meyer, G. Mittag, J. Mnich, A. Mussgiller, E. Ntomari, D. Pitzl, A. Raspereza, B. Roland, M. Savitskyi, P. Saxena, R. Shevchenko, S. Spannagel, N. Stefaniuk, G.P. Van Onsem, R. Walsh, Y. Wen, K. Wichmann, C. Wissing, O. Zenaiev

University of Hamburg, Hamburg, Germany

R. Aggleton, S. Bein, V. Blobel, M. Centis Vignali, T. Dreyer, E. Garutti, D. Gonzalez, J. Haller, A. Hinzmann, M. Hoffmann, A. Karavdina, R. Klanner, R. Kogler, N. Kovalchuk, S. Kurz, T. Lapsien, I. Marchesini, D. Marconi, M. Meyer, M. Niedziela, D. Nowatschin, F. Pantaleo¹⁵, T. Peiffer, A. Perieanu, C. Scharf, P. Schleper, A. Schmidt, S. Schumann, J. Schwandt, J. Sonneveld, H. Stadie, G. Steinbrück, F.M. Stober, M. Stöver, H. Tholen, D. Troendle, E. Usai, L. Vanelderen, A. Vanhoefer, B. Vormwald

Institut für Experimentelle Kernphysik, Karlsruhe, Germany

M. Akbiyik, C. Barth, M. Baselga, S. Baur, E. Butz, R. Caspart, T. Chwalek, F. Colombo, W. De Boer, A. Dierlamm, N. Faltermann, B. Freund, R. Friese, M. Giffels, D. Haitz, M.A. Harrendorf, F. Hartmann¹⁵, S.M. Heindl, U. Husemann, F. Kassel¹⁵, S. Kudella, H. Mildner, M.U. Mozer, Th. Müller, M. Plagge, G. Quast, K. Rabbertz, M. Schröder, I. Shvetsov, G. Sieber, H.J. Simonis, R. Ulrich, S. Wayand, M. Weber, T. Weiler, S. Williamson, C. Wöhrmann, R. Wolf

Institute of Nuclear and Particle Physics (INPP), NCSR Demokritos, Aghia Paraskevi, Greece

G. Anagnostou, G. Daskalakis, T. Gerasis, V.A. Giakoumopoulou, A. Kyriakis, D. Loukas, I. Topsis-Giotis

National and Kapodistrian University of Athens, Athens, Greece

G. Karathanasis, S. Kesisoglou, A. Panagiotou, N. Saoulidou

National Technical University of Athens, Athens, Greece

K. Kousouris

University of Ioánnina, Ioánnina, Greece

I. Evangelou, C. Foudas, P. Kokkas, S. Mallios, N. Manthos, I. Papadopoulos, E. Paradas, J. Strologas, F.A. Triantis

MTA-ELTE Lendület CMS Particle and Nuclear Physics Group, Eötvös Loránd University, Budapest, Hungary

M. Csanad, N. Filipovic, G. Pasztor, O. Surányi, G.I. Veres¹⁹

Wigner Research Centre for Physics, Budapest, Hungary

G. Bencze, C. Hajdu, D. Horvath²⁰, Á. Hunyadi, F. Sikler, V. Veszpremi, A.J. Zsigmond

Institute of Nuclear Research ATOMKI, Debrecen, Hungary

N. Beni, S. Czellar, J. Karancsi²¹, A. Makovec, J. Molnar, Z. Szillasi

Institute of Physics, University of Debrecen, Debrecen, Hungary

M. Bartók¹⁹, P. Raics, Z.L. Trocsanyi, B. Ujvari

Indian Institute of Science (IISc), Bangalore, India

S. Choudhury, J.R. Komaragiri

National Institute of Science Education and Research, Bhubaneswar, IndiaS. Bahinipati²², S. Bhowmik, P. Mal, K. Mandal, A. Nayak²³, D.K. Sahoo²², N. Sahoo, S.K. Swain**Panjab University, Chandigarh, India**

S. Bansal, S.B. Beri, V. Bhatnagar, R. Chawla, N. Dhingra, A.K. Kalsi, A. Kaur, M. Kaur, S. Kaur, R. Kumar, P. Kumari, A. Mehta, J.B. Singh, G. Walia

University of Delhi, Delhi, India

Ashok Kumar, Aashaq Shah, A. Bhardwaj, S. Chauhan, B.C. Choudhary, R.B. Garg, S. Keshri, A. Kumar, S. Malhotra, M. Naimuddin, K. Ranjan, R. Sharma

Saha Institute of Nuclear Physics, HBNI, Kolkata, India

R. Bhardwaj, R. Bhattacharya, S. Bhattacharya, U. Bhawandeep, S. Dey, S. Dutt, S. Dutta, S. Ghosh, N. Majumdar, A. Modak, K. Mondal, S. Mukhopadhyay, S. Nandan, A. Purohit, A. Roy, D. Roy, S. Roy Chowdhury, S. Sarkar, M. Sharan, S. Thakur

Indian Institute of Technology Madras, Madras, India

P.K. Behera

Bhabha Atomic Research Centre, Mumbai, IndiaR. Chudasama, D. Dutta, V. Jha, V. Kumar, A.K. Mohanty¹⁵, P.K. Netrakanti, L.M. Pant, P. Shukla, A. Topkar**Tata Institute of Fundamental Research-A, Mumbai, India**

T. Aziz, S. Dugad, B. Mahakud, S. Mitra, G.B. Mohanty, N. Sur, B. Sutar

Tata Institute of Fundamental Research-B, Mumbai, IndiaS. Banerjee, S. Bhattacharya, S. Chatterjee, P. Das, M. Guchait, Sa. Jain, S. Kumar, M. Maity²⁴, G. Majumder, K. Mazumdar, T. Sarkar²⁴, N. Wickramage²⁵**Indian Institute of Science Education and Research (IISER), Pune, India**

S. Chauhan, S. Dube, V. Hegde, A. Kapoor, K. Kothekar, S. Pandey, A. Rane, S. Sharma

Institute for Research in Fundamental Sciences (IPM), Tehran, IranS. Chenarani²⁶, E. Eskandari Tadavani, S.M. Etesami²⁶, M. Khakzad, M. Mohammadi Najafabadi, M. Naseri, S. Paktinat Mehdiabadi²⁷, F. Rezaei Hosseinabadi, B. Safarzadeh²⁸, M. Zeinali**University College Dublin, Dublin, Ireland**

M. Felcini, M. Grunewald

INFN Sezione di Bari ^a, Università di Bari ^b, Politecnico di Bari ^c, Bari, ItalyM. Abbrescia^{a,b}, C. Calabria^{a,b}, A. Colaleo^a, D. Creanza^{a,c}, L. Cristella^{a,b}, N. De Filippis^{a,c}, M. De Palma^{a,b}, F. Errico^{a,b}, L. Fiore^a, G. Iaselli^{a,c}, S. Lezki^{a,b}, G. Maggi^{a,c}, M. Maggi^a, G. Miniello^{a,b}, S. My^{a,b}, S. Nuzzo^{a,b}, A. Pompili^{a,b}, G. Pugliese^{a,c}, R. Radogna^a, A. Ranieri^a, G. Selvaggi^{a,b}, A. Sharma^a, L. Silvestris^{a,15}, R. Venditti^a, P. Verwilligen^a**INFN Sezione di Bologna ^a, Università di Bologna ^b, Bologna, Italy**G. Abbiendi^a, C. Battilana^{a,b}, D. Bonacorsi^{a,b}, L. Borgonovi^{a,b}, S. Braibant-Giacomelli^{a,b}, R. Campanini^{a,b}, P. Capiluppi^{a,b}, A. Castro^{a,b}, F.R. Cavallo^a, S.S. Chhibra^a, G. Codispoti^{a,b}, M. Cuffiani^{a,b}, G.M. Dallavalle^a, F. Fabbri^a, A. Fanfani^{a,b}, D. Fasanella^{a,b}, P. Giacomelli^a, C. Grandi^a, L. Guiducci^{a,b}, S. Marcellini^a, G. Masetti^a, A. Montanari^a, F.L. Navarria^{a,b}, A. Perrotta^a, A.M. Rossi^{a,b}, T. Rovelli^{a,b}, G.P. Siroli^{a,b}, N. Tosi^a

INFN Sezione di Catania ^a, Università di Catania ^b, Catania, Italy

S. Albergo^{a,b}, S. Costa^{a,b}, A. Di Mattia^a, F. Giordano^{a,b}, R. Potenza^{a,b}, A. Tricomi^{a,b}, C. Tuve^{a,b}

INFN Sezione di Firenze ^a, Università di Firenze ^b, Firenze, Italy

G. Barbagli^a, K. Chatterjee^{a,b}, V. Ciulli^{a,b}, C. Civinini^a, R. D'Alessandro^{a,b}, E. Focardi^{a,b}, P. Lenzi^{a,b}, M. Meschini^a, S. Paoletti^a, L. Russo^{a,29}, G. Sguazzoni^a, D. Strom^a, L. Viliani^{a,b,15}

INFN Laboratori Nazionali di Frascati, Frascati, Italy

L. Benussi, S. Bianco, F. Fabbri, D. Piccolo, F. Primavera¹⁵

INFN Sezione di Genova ^a, Università di Genova ^b, Genova, Italy

V. Calvelli^{a,b}, F. Ferro^a, E. Robutti^a, S. Tosi^{a,b}

INFN Sezione di Milano-Bicocca ^a, Università di Milano-Bicocca ^b, Milano, Italy

A. Benaglia^a, A. Beschi, L. Brianza^{a,b}, F. Brivio^{a,b}, V. Ciriolo^{a,b}, M.E. Dinardo^{a,b}, S. Fiorendi^{a,b}, S. Gennai^a, A. Ghezzi^{a,b}, P. Govoni^{a,b}, M. Malberti^{a,b}, S. Malvezzi^a, R.A. Manzoni^{a,b}, D. Menasce^a, L. Moroni^a, M. Paganoni^{a,b}, K. Pauwels^{a,b}, D. Pedrini^a, S. Pigazzini^{a,b,30}, S. Ragazzi^{a,b}, N. Redaelli^a, T. Tabarelli de Fatis^{a,b}

INFN Sezione di Napoli ^a, Università di Napoli 'Federico II' ^b, Napoli, Italy, Università della Basilicata ^c, Potenza, Italy, Università G. Marconi ^d, Roma, Italy

S. Buontempo^a, N. Cavallo^{a,c}, S. Di Guida^{a,d,15}, F. Fabozzi^{a,c}, F. Fienga^{a,b}, A.O.M. Iorio^{a,b}, W.A. Khan^a, L. Lista^a, S. Meola^{a,d,15}, P. Paolucci^{a,15}, C. Sciacca^{a,b}, F. Thyssen^a

INFN Sezione di Padova ^a, Università di Padova ^b, Padova, Italy, Università di Trento ^c, Trento, Italy

P. Azzi^a, N. Bacchetta^a, L. Benato^{a,b}, D. Bisello^{a,b}, A. Boletti^{a,b}, R. Carlin^{a,b}, P. Checchia^a, M. Dall'Osso^{a,b}, P. De Castro Manzano^a, T. Dorigo^a, F. Gasparini^{a,b}, U. Gasparini^{a,b}, A. Gozzelino^a, S. Lacaprara^a, P. Lujan, M. Margoni^{a,b}, A.T. Meneguzzo^{a,b}, N. Pozzobon^{a,b}, P. Ronchese^{a,b}, R. Rossin^{a,b}, F. Simonetto^{a,b}, E. Torassa^a, S. Ventura^a, M. Zanetti^{a,b}, P. Zotto^{a,b}, G. Zumerle^{a,b}

INFN Sezione di Pavia ^a, Università di Pavia ^b, Pavia, Italy

A. Braghieri^a, A. Magnani^a, P. Montagna^{a,b}, S.P. Ratti^{a,b}, V. Re^a, M. Ressegotti^{a,b}, C. Riccardi^{a,b}, P. Salvini^a, I. Vai^{a,b}, P. Vitulo^{a,b}

INFN Sezione di Perugia ^a, Università di Perugia ^b, Perugia, Italy

L. Alunni Solestizi^{a,b}, M. Biasini^{a,b}, G.M. Bilei^a, C. Cecchi^{a,b}, D. Ciangottini^{a,b}, L. Fanò^{a,b}, P. Lariccia^{a,b}, R. Leonardi^{a,b}, E. Manoni^a, G. Mantovani^{a,b}, V. Mariani^{a,b}, M. Menichelli^a, A. Rossi^{a,b}, A. Santocchia^{a,b}, D. Spiga^a

INFN Sezione di Pisa ^a, Università di Pisa ^b, Scuola Normale Superiore di Pisa ^c, Pisa, Italy

K. Androsov^a, P. Azzurri^{a,15}, G. Bagliesi^a, T. Boccali^a, L. Borrello, R. Castaldi^a, M.A. Ciocci^{a,b}, R. Dell'Orso^a, G. Fedi^a, L. Giannini^{a,c}, A. Giassi^a, M.T. Grippo^{a,29}, F. Ligabue^{a,c}, T. Lomtadze^a, E. Manca^{a,c}, G. Mandorli^{a,c}, L. Martini^{a,b}, A. Messineo^{a,b}, F. Palla^a, A. Rizzi^{a,b}, A. Savoy-Navarro^{a,31}, P. Spagnolo^a, R. Tenchini^a, G. Tonelli^{a,b}, A. Venturi^a, P.G. Verdini^a

INFN Sezione di Roma ^a, Sapienza Università di Roma ^b, Rome, Italy

L. Barone^{a,b}, F. Cavallari^a, M. Cipriani^{a,b}, N. Daci^a, D. Del Re^{a,b,15}, E. Di Marco^{a,b}, M. Diemoz^a, S. Gelli^{a,b}, E. Longo^{a,b}, F. Margaroli^{a,b}, B. Marzocchi^{a,b}, P. Meridiani^a, G. Organtini^{a,b}, R. Paramatti^{a,b}, F. Preiato^{a,b}, S. Rahatlou^{a,b}, C. Rovelli^a, F. Santanastasio^{a,b}

INFN Sezione di Torino ^a, Università di Torino ^b, Torino, Italy, Università del Piemonte Orientale ^c, Novara, Italy

N. Amapane^{a,b}, R. Arcidiacono^{a,c}, S. Argiro^{a,b}, M. Arneodo^{a,c}, N. Bartosik^a, R. Bellan^{a,b},

C. Biino^a, N. Cartiglia^a, F. Cenna^{a,b}, M. Costa^{a,b}, R. Covarelli^{a,b}, A. Degano^{a,b}, N. Demaria^a, B. Kiani^{a,b}, C. Mariotti^a, S. Maselli^a, E. Migliore^{a,b}, V. Monaco^{a,b}, E. Monteil^{a,b}, M. Monteno^a, M.M. Obertino^{a,b}, L. Pacher^{a,b}, N. Pastrone^a, M. Pelliccioni^a, G.L. Pinna Angioni^{a,b}, F. Ravera^{a,b}, A. Romero^{a,b}, M. Ruspa^{a,c}, R. Sacchi^{a,b}, K. Shchelina^{a,b}, V. Sola^a, A. Solano^{a,b}, A. Staiano^a, P. Traczyk^{a,b}

INFN Sezione di Trieste^a, Università di Trieste^b, Trieste, Italy
S. Belforte^a, M. Casarsa^a, F. Cossutti^a, G. Della Ricca^{a,b}, A. Zanetti^a

Kyungpook National University, Daegu, Korea

D.H. Kim, G.N. Kim, M.S. Kim, J. Lee, S. Lee, S.W. Lee, C.S. Moon, Y.D. Oh, S. Sekmen, D.C. Son, Y.C. Yang

Chonbuk National University, Jeonju, Korea

A. Lee

Chonnam National University, Institute for Universe and Elementary Particles, Kwangju, Korea

H. Kim, D.H. Moon, G. Oh

Hanyang University, Seoul, Korea

J.A. Brochero Cifuentes, J. Goh, T.J. Kim

Korea University, Seoul, Korea

S. Cho, S. Choi, Y. Go, D. Gyun, S. Ha, B. Hong, Y. Jo, Y. Kim, K. Lee, K.S. Lee, S. Lee, J. Lim, S.K. Park, Y. Roh

Seoul National University, Seoul, Korea

J. Almond, J. Kim, J.S. Kim, H. Lee, K. Lee, K. Nam, S.B. Oh, B.C. Radburn-Smith, S.h. Seo, U.K. Yang, H.D. Yoo, G.B. Yu

University of Seoul, Seoul, Korea

M. Choi, H. Kim, J.H. Kim, J.S.H. Lee, I.C. Park

Sungkyunkwan University, Suwon, Korea

Y. Choi, C. Hwang, J. Lee, I. Yu

Vilnius University, Vilnius, Lithuania

V. Dudenas, A. Juodagalvis, J. Vaitkus

National Centre for Particle Physics, Universiti Malaya, Kuala Lumpur, Malaysia

I. Ahmed, Z.A. Ibrahim, M.A.B. Md Ali³², F. Mohamad Idris³³, W.A.T. Wan Abdullah, M.N. Yusli, Z. Zolkapli

Centro de Investigacion y de Estudios Avanzados del IPN, Mexico City, Mexico

Reyes-Almanza, R, Ramirez-Sanchez, G., Duran-Osuna, M. C., H. Castilla-Valdez, E. De La Cruz-Burelo, I. Heredia-De La Cruz³⁴, Rabadan-Trejo, R. I., R. Lopez-Fernandez, J. Mejia Guisao, A. Sanchez-Hernandez

Universidad Iberoamericana, Mexico City, Mexico

S. Carrillo Moreno, C. Oropeza Barrera, F. Vazquez Valencia

Benemerita Universidad Autonoma de Puebla, Puebla, Mexico

I. Pedraza, H.A. Salazar Ibarguen, C. Uribe Estrada

Universidad Autónoma de San Luis Potosí, San Luis Potosí, Mexico

A. Morelos Pineda

University of Auckland, Auckland, New Zealand

D. Krofcheck

University of Canterbury, Christchurch, New Zealand

P.H. Butler

National Centre for Physics, Quaid-I-Azam University, Islamabad, Pakistan

A. Ahmad, M. Ahmad, Q. Hassan, H.R. Hoorani, A. Saddique, M.A. Shah, M. Shoaib, M. Waqas

National Centre for Nuclear Research, Swierk, Poland

H. Bialkowska, M. Bluj, B. Boimska, T. Frueboes, M. Górski, M. Kazana, K. Nawrocki, M. Szleper, P. Zalewski

Institute of Experimental Physics, Faculty of Physics, University of Warsaw, Warsaw, PolandK. Bunkowski, A. Byszuk³⁵, K. Doroba, A. Kalinowski, M. Konecki, J. Krolikowski, M. Misiura, M. Olszewski, A. Pyskir, M. Walczak**Laboratório de Instrumentação e Física Experimental de Partículas, Lisboa, Portugal**

P. Bargassa, C. Beirão Da Cruz E Silva, A. Di Francesco, P. Faccioli, B. Galinhas, M. Gallinaro, J. Hollar, N. Leonardo, L. Lloret Iglesias, M.V. Nemallapudi, J. Seixas, G. Strong, O. Toldaiev, D. Vadrucio, J. Varela

Joint Institute for Nuclear Research, Dubna, RussiaV. Alexakhin, P. Bunin, A. Golunov, I. Golutvin, N. Gorbounov, I. Gorbunov, A. Kamenev, V. Karjavin, A. Lanev, A. Malakhov, V. Matveev^{36,37}, V. Palichik, V. Perelygin, M. Savina, S. Shmatov, N. Skatchkov, V. Smirnov, A. Zarubin**Petersburg Nuclear Physics Institute, Gatchina (St. Petersburg), Russia**Y. Ivanov, V. Kim³⁸, E. Kuznetsova³⁹, P. Levchenko, V. Murzin, V. Oreshkin, I. Smirnov, V. Sulimov, L. Uvarov, S. Vavilov, A. Vorobyev**Institute for Nuclear Research, Moscow, Russia**

Yu. Andreev, A. Dermenev, S. Gninenko, N. Golubev, A. Karneyeu, M. Kirsanov, N. Krasnikov, A. Pashenkov, D. Tlisov, A. Toropin

Institute for Theoretical and Experimental Physics, Moscow, Russia

V. Epshteyn, V. Gavrilov, N. Lychkovskaya, V. Popov, I. Pozdnyakov, G. Safronov, A. Spiridonov, A. Stepenov, M. Toms, E. Vlasov, A. Zhokin

Moscow Institute of Physics and Technology, Moscow, RussiaT. Aushev, A. Bylinkin³⁷**National Research Nuclear University 'Moscow Engineering Physics Institute' (MEPhI), Moscow, Russia**M. Chadeeva⁴⁰, P. Parygin, D. Philippov, S. Polikarpov, E. Popova, V. Rusinov**P.N. Lebedev Physical Institute, Moscow, Russia**V. Andreev, M. Azarkin³⁷, I. Dremin³⁷, M. Kirakosyan³⁷, A. Terkulov**Skobeltsyn Institute of Nuclear Physics, Lomonosov Moscow State University, Moscow, Russia**A. Baskakov, A. Belyaev, E. Boos, M. Dubinin⁴¹, L. Dudko, A. Ershov, A. Gribushin, V. Klyukhin, O. Kodolova, I. Lokhtin, I. Miagkov, S. Obraztsov, S. Petrushanko, V. Savrin, A. Snigirev

Novosibirsk State University (NSU), Novosibirsk, RussiaV. Blinov⁴², D. Shtol⁴², Y. Skovpen⁴²**State Research Center of Russian Federation, Institute for High Energy Physics, Protvino, Russia**

I. Azhgirey, I. Bayshev, S. Bitioukov, D. Elumakhov, V. Kachanov, A. Kalinin, D. Konstantinov, P. Mandrik, V. Petrov, R. Ryutin, A. Sobol, S. Troshin, N. Tyurin, A. Uzunian, A. Volkov

University of Belgrade, Faculty of Physics and Vinca Institute of Nuclear Sciences, Belgrade, SerbiaP. Adzic⁴³, P. Cirkovic, D. Devetak, M. Dordevic, J. Milosevic, V. Rekovic**Centro de Investigaciones Energéticas Medioambientales y Tecnológicas (CIEMAT), Madrid, Spain**

J. Alcaraz Maestre, M. Barrio Luna, M. Cerrada, N. Colino, B. De La Cruz, A. Delgado Peris, A. Escalante Del Valle, C. Fernandez Bedoya, J.P. Fernández Ramos, J. Flix, M.C. Fouz, O. Gonzalez Lopez, S. Goy Lopez, J.M. Hernandez, M.I. Josa, D. Moran, A. Pérez-Calero Yzquierdo, J. Puerta Pelayo, A. Quintario Olmeda, I. Redondo, L. Romero, M.S. Soares, A. Álvarez Fernández

Universidad Autónoma de Madrid, Madrid, Spain

C. Albajar, J.F. de Trocóniz, M. Missiroli

Universidad de Oviedo, Oviedo, Spain

J. Cuevas, C. Erice, J. Fernandez Menendez, I. Gonzalez Caballero, J.R. González Fernández, E. Palencia Cortezon, S. Sanchez Cruz, P. Vischia, J.M. Vizan Garcia

Instituto de Física de Cantabria (IFCA), CSIC-Universidad de Cantabria, Santander, Spain

I.J. Cabrillo, A. Calderon, B. Chazin Quero, E. Curras, J. Duarte Campderros, M. Fernandez, J. Garcia-Ferrero, G. Gomez, A. Lopez Virto, J. Marco, C. Martinez Rivero, P. Martinez Ruiz del Arbol, F. Matorras, J. Piedra Gomez, T. Rodrigo, A. Ruiz-Jimeno, L. Scodellaro, N. Trevisani, I. Vila, R. Vilar Cortabitarte

CERN, European Organization for Nuclear Research, Geneva, SwitzerlandD. Abbaneo, B. Akgun, E. Auffray, P. Baillon, A.H. Ball, D. Barney, J. Bendavid, M. Bianco, P. Bloch, A. Bocci, C. Botta, T. Camporesi, R. Castello, M. Cepeda, G. Cerminara, E. Chapon, Y. Chen, D. d'Enterria, A. Dabrowski, V. Daponte, A. David, M. De Gruttola, A. De Roeck, N. Deelen, M. Dobson, T. du Pree, M. Dünser, N. Dupont, A. Elliott-Peisert, P. Everaerts, F. Fallavollita, G. Franzoni, J. Fulcher, W. Funk, D. Gigi, A. Gilbert, K. Gill, F. Glege, D. Gulhan, P. Harris, J. Hegeman, V. Innocente, A. Jafari, P. Janot, O. Karacheban¹⁸, J. Kieseler, V. Knünz, A. Kornmayer, M.J. Kortelainen, M. Krammer¹, C. Lange, P. Lecoq, C. Lourenço, M.T. Lucchini, L. Malgeri, M. Mannelli, A. Martelli, F. Meijers, J.A. Merlin, S. Mersi, E. Meschi, P. Milenovic⁴⁴, F. Moortgat, M. Mulders, H. Neugebauer, J. Ngadiuba, S. Orfanelli, L. Orsini, L. Pape, E. Perez, M. Peruzzi, A. Petrilli, G. Petrucciani, A. Pfeiffer, M. Pierini, D. Rabady, A. Racz, T. Reis, G. Rolandi⁴⁵, M. Rovere, H. Sakulin, C. Schäfer, C. Schwick, M. Seidel, M. Selvaggi, A. Sharma, P. Silva, P. Sphicas⁴⁶, A. Stakia, J. Steggemann, M. Stoye, M. Tosi, D. Treille, A. Triossi, A. Tsirou, V. Veckalns⁴⁷, M. Verweij, W.D. Zeuner**Paul Scherrer Institut, Villigen, Switzerland**W. Bertl[†], L. Caminada⁴⁸, K. Deiters, W. Erdmann, R. Horisberger, Q. Ingram, H.C. Kaestli, D. Kotlinski, U. Langenegger, T. Rohe, S.A. Wiederkehr**ETH Zurich - Institute for Particle Physics and Astrophysics (IPA), Zurich, Switzerland**

M. Backhaus, L. Bäni, P. Berger, L. Bianchini, B. Casal, G. Dissertori, M. Dittmar, M. Donegà,

C. Dorfer, C. Grab, C. Heidegger, D. Hits, J. Hoss, G. Kasieczka, T. Klijsma, W. Lustermann, B. Mangano, M. Marionneau, M.T. Meinhard, D. Meister, F. Micheli, P. Musella, F. Nessi-Tedaldi, F. Pandolfi, J. Pata, F. Pauss, G. Perrin, L. Perrozzi, M. Quittnat, M. Reichmann, D.A. Sanz Becerra, M. Schönenberger, L. Shchutska, V.R. Tavolaro, K. Theofilatos, M.L. Vesterbacka Olsson, R. Wallny, D.H. Zhu

Universität Zürich, Zurich, Switzerland

T.K. Aarrestad, C. AMSler⁴⁹, M.F. Canelli, A. De Cosa, R. Del Burgo, S. Donato, C. Galloni, T. Hreus, B. Kilminster, D. Pinna, G. Rauco, P. Robmann, D. Salerno, K. Schweiger, C. Seitz, Y. Takahashi, A. Zucchetta

National Central University, Chung-Li, Taiwan

V. Candelise, T.H. Doan, Sh. Jain, R. Khurana, C.M. Kuo, W. Lin, A. Pozdnyakov, S.S. Yu

National Taiwan University (NTU), Taipei, Taiwan

Arun Kumar, P. Chang, Y. Chao, K.F. Chen, P.H. Chen, F. Fiori, W.-S. Hou, Y. Hsiung, Y.F. Liu, R.-S. Lu, E. Paganis, A. Psallidas, A. Steen, J.f. Tsai

Chulalongkorn University, Faculty of Science, Department of Physics, Bangkok, Thailand

B. Asavapibhop, K. Kovitanggoon, G. Singh, N. Srimanobhas

Çukurova University, Physics Department, Science and Art Faculty, Adana, Turkey

M.N. Bakirci⁵⁰, F. Boran, S. Damarseckin, Z.S. Demiroglu, C. Dozen, I. Dumanoglu, E. Eskut, S. Girgis, G. Gokbulut, Y. Guler, I. Hos⁵¹, E.E. Kangal⁵², O. Kara, U. Kiminsu, M. Oglakci, G. Onengut⁵³, K. Ozdemir⁵⁴, S. Ozturk⁵⁰, H. Topakli⁵⁰, S. Turkcapar, I.S. Zorbakir, C. Zorbilmez

Middle East Technical University, Physics Department, Ankara, Turkey

B. Bilin, G. Karapinar⁵⁵, K. Ocalan⁵⁶, M. Yalvac, M. Zeyrek

Bogazici University, Istanbul, Turkey

E. Gülmez, M. Kaya⁵⁷, O. Kaya⁵⁸, S. Tekten, E.A. Yetkin⁵⁹

Istanbul Technical University, Istanbul, Turkey

M.N. Agaras, S. Atay, A. Cakir, K. Cankocak

Institute for Scintillation Materials of National Academy of Science of Ukraine, Kharkov, Ukraine

B. Grynyov

National Scientific Center, Kharkov Institute of Physics and Technology, Kharkov, Ukraine

L. Levchuk

University of Bristol, Bristol, United Kingdom

F. Ball, L. Beck, J.J. Brooke, D. Burns, E. Clement, D. Cussans, O. Davignon, H. Flacher, J. Goldstein, G.P. Heath, H.F. Heath, J. Jacob, L. Kreczko, D.M. Newbold⁶⁰, S. Paramesvaran, T. Sakuma, S. Seif El Nasr-storey, D. Smith, V.J. Smith

Rutherford Appleton Laboratory, Didcot, United Kingdom

K.W. Bell, A. Belyaev⁶¹, C. Brew, R.M. Brown, L. Calligaris, D. Cieri, D.J.A. Cockerill, J.A. Coughlan, K. Harder, S. Harper, E. Olaiya, D. Petyt, C.H. Shepherd-Themistocleous, A. Thea, I.R. Tomalin, T. Williams

Imperial College, London, United Kingdom

G. Auzinger, R. Bainbridge, J. Borg, S. Breeze, O. Buchmuller, A. Bundock, S. Casasso, M. Citron, D. Colling, L. Corpe, P. Dauncey, G. Davies, A. De Wit, M. Della Negra, R. Di Maria, A. Elwood, Y. Haddad, G. Hall, G. Iles, T. James, R. Lane, C. Laner, L. Lyons, A.-M. Magnan,

S. Malik, L. Mastrolorenzo, T. Matsushita, J. Nash, A. Nikitenko⁷, V. Palladino, M. Pesaresi, D.M. Raymond, A. Richards, A. Rose, E. Scott, C. Seez, A. Shtipliyski, S. Summers, A. Tapper, K. Uchida, M. Vazquez Acosta⁶², T. Virdee¹⁵, N. Wardle, D. Winterbottom, J. Wright, S.C. Zenz

Brunel University, Uxbridge, United Kingdom

J.E. Cole, P.R. Hobson, A. Khan, P. Kyberd, I.D. Reid, P. Symonds, L. Teodorescu, M. Turner, S. Zahid

Baylor University, Waco, USA

A. Borzou, K. Call, J. Dittmann, K. Hatakeyama, H. Liu, N. Pastika, C. Smith

Catholic University of America, Washington DC, USA

R. Bartek, A. Dominguez

The University of Alabama, Tuscaloosa, USA

A. Buccilli, S.I. Cooper, C. Henderson, P. Rumerio, C. West

Boston University, Boston, USA

D. Arcaro, A. Avetisyan, T. Bose, D. Gastler, D. Rankin, C. Richardson, J. Rohlf, L. Sulak, D. Zou

Brown University, Providence, USA

G. Benelli, D. Cutts, A. Garabedian, M. Hadley, J. Hakala, U. Heintz, J.M. Hogan, K.H.M. Kwok, E. Laird, G. Landsberg, J. Lee, Z. Mao, M. Narain, J. Pazzini, S. Piperov, S. Sagir, R. Syarif, D. Yu

University of California, Davis, Davis, USA

R. Band, C. Brainerd, R. Breedon, D. Burns, M. Calderon De La Barca Sanchez, M. Chertok, J. Conway, R. Conway, P.T. Cox, R. Erbacher, C. Flores, G. Funk, M. Gardner, W. Ko, R. Lander, C. Mclean, M. Mulhearn, D. Pellett, J. Pilot, S. Shalhout, M. Shi, J. Smith, D. Stolp, K. Tos, M. Tripathi, Z. Wang

University of California, Los Angeles, USA

M. Bachtis, C. Bravo, R. Cousins, A. Dasgupta, A. Florent, J. Hauser, M. Ignatenko, N. Mccoll, S. Regnard, D. Saltzberg, C. Schnaible, V. Valuev

University of California, Riverside, Riverside, USA

E. Bouvier, K. Burt, R. Clare, J. Ellison, J.W. Gary, S.M.A. Ghiasi Shirazi, G. Hanson, J. Heilman, E. Kennedy, F. Lacroix, O.R. Long, M. Olmedo Negrete, M.I. Paneva, W. Si, L. Wang, H. Wei, S. Wimpenny, B. R. Yates

University of California, San Diego, La Jolla, USA

J.G. Branson, S. Cittolin, M. Derdzinski, R. Gerosa, D. Gilbert, B. Hashemi, A. Holzner, D. Klein, G. Kole, V. Krutelyov, J. Letts, I. Macneill, M. Masciovecchio, D. Olivito, S. Padhi, M. Pieri, M. Sani, V. Sharma, S. Simon, M. Tadel, A. Vartak, S. Wasserbaech⁶³, J. Wood, F. Würthwein, A. Yagil, G. Zevi Della Porta

University of California, Santa Barbara - Department of Physics, Santa Barbara, USA

N. Amin, R. Bhandari, J. Bradmiller-Feld, C. Campagnari, A. Dishaw, V. Dutta, M. Franco Sevilla, C. George, F. Golf, L. Gouskos, J. Gran, R. Heller, J. Incandela, S.D. Mullin, A. Ovcharova, H. Qu, J. Richman, D. Stuart, I. Suarez, J. Yoo

California Institute of Technology, Pasadena, USA

D. Anderson, A. Bornheim, J.M. Lawhorn, H.B. Newman, T. Nguyen, C. Pena, M. Spiropulu, J.R. Vlimant, S. Xie, Z. Zhang, R.Y. Zhu

Carnegie Mellon University, Pittsburgh, USA

M.B. Andrews, T. Ferguson, T. Mudholkar, M. Paulini, J. Russ, M. Sun, H. Vogel, I. Vorobiev, M. Weinberg

University of Colorado Boulder, Boulder, USA

J.P. Cumalat, W.T. Ford, F. Jensen, A. Johnson, M. Krohn, S. Leontsinis, T. Mulholland, K. Stenson, S.R. Wagner

Cornell University, Ithaca, USA

J. Alexander, J. Chaves, J. Chu, S. Dittmer, K. Mcdermott, N. Mirman, J.R. Patterson, D. Quach, A. Rinkevicius, A. Ryd, L. Skinnari, L. Soffi, S.M. Tan, Z. Tao, J. Thom, J. Tucker, P. Wittich, M. Zientek

Fermi National Accelerator Laboratory, Batavia, USA

S. Abdullin, M. Albrow, M. Alyari, G. Apollinari, A. Apresyan, A. Apyan, S. Banerjee, L.A.T. Bauerdick, A. Beretvas, J. Berryhill, P.C. Bhat, G. Bolla[†], K. Burkett, J.N. Butler, A. Canepa, G.B. Cerati, H.W.K. Cheung, F. Chlebana, M. Cremonesi, J. Duarte, V.D. Elvira, J. Freeman, Z. Gecse, E. Gottschalk, L. Gray, D. Green, S. Grünendahl, O. Gutsche, R.M. Harris, S. Hasegawa, J. Hirschauer, Z. Hu, B. Jayatilaka, S. Jindariani, M. Johnson, U. Joshi, B. Klima, B. Kreis, S. Lammel, D. Lincoln, R. Lipton, M. Liu, T. Liu, R. Lopes De Sá, J. Lykken, K. Maeshima, N. Magini, J.M. Marraffino, D. Mason, P. McBride, P. Merkel, S. Mrenna, S. Nahn, V. O'Dell, K. Pedro, O. Prokofyev, G. Rakness, L. Ristori, B. Schneider, E. Sexton-Kennedy, A. Soha, W.J. Spalding, L. Spiegel, S. Stoynev, J. Strait, N. Strobbe, L. Taylor, S. Tkaczyk, N.V. Tran, L. Uplegger, E.W. Vaandering, C. Vernieri, M. Verzocchi, R. Vidal, M. Wang, H.A. Weber, A. Whitbeck

University of Florida, Gainesville, USA

D. Acosta, P. Avery, P. Bortignon, D. Bourilkov, A. Brinkerhoff, A. Carnes, M. Carver, D. Curry, R.D. Field, I.K. Furic, S.V. Gleyzer, B.M. Joshi, J. Konigsberg, A. Korytov, K. Kotov, P. Ma, K. Matchev, H. Mei, G. Mitselmakher, D. Rank, K. Shi, D. Sperka, N. Terentyev, L. Thomas, J. Wang, S. Wang, J. Yelton

Florida International University, Miami, USA

Y.R. Joshi, S. Linn, P. Markowitz, J.L. Rodriguez

Florida State University, Tallahassee, USA

A. Ackert, T. Adams, A. Askew, S. Hagopian, V. Hagopian, K.F. Johnson, T. Kolberg, G. Martinez, T. Perry, H. Prosper, A. Saha, A. Santra, V. Sharma, R. Yohay

Florida Institute of Technology, Melbourne, USA

M.M. Baarmand, V. Bhopatkar, S. Colafranceschi, M. Hohlmann, D. Noonan, T. Roy, F. Yumiceva

University of Illinois at Chicago (UIC), Chicago, USA

M.R. Adams, L. Apanasevich, D. Berry, R.R. Betts, R. Cavanaugh, X. Chen, O. Evdokimov, C.E. Gerber, D.A. Hangal, D.J. Hofman, K. Jung, J. Kamin, I.D. Sandoval Gonzalez, M.B. Tonjes, H. Trauger, N. Varelas, H. Wang, Z. Wu, J. Zhang

The University of Iowa, Iowa City, USA

B. Bilki⁶⁴, W. Clarida, K. Dilsiz⁶⁵, S. Durgut, R.P. Gandrajula, M. Haytmyradov, V. Khristenko, J.-P. Merlo, H. Mermerkaya⁶⁶, A. Mestvirishvili, A. Moeller, J. Nachtman, H. Ogul⁶⁷, Y. Onel, F. Ozok⁶⁸, A. Penzo, C. Snyder, E. Tiras, J. Wetzel, K. Yi

Johns Hopkins University, Baltimore, USA

B. Blumenfeld, A. Cocoros, N. Eminizer, D. Fehling, L. Feng, A.V. Gritsan, P. Maksimovic, J. Roskes, U. Sarica, M. Swartz, M. Xiao, C. You

The University of Kansas, Lawrence, USA

A. Al-bataineh, P. Baringer, A. Bean, S. Boren, J. Bowen, J. Castle, S. Khalil, A. Kropivnitskaya, D. Majumder, W. Mcbrayer, M. Murray, C. Royon, S. Sanders, E. Schmitz, J.D. Tapia Takaki, Q. Wang

Kansas State University, Manhattan, USA

A. Ivanov, K. Kaadze, Y. Maravin, A. Mohammadi, L.K. Saini, N. Skhirtladze, S. Toda

Lawrence Livermore National Laboratory, Livermore, USA

F. Rebassoo, D. Wright

University of Maryland, College Park, USA

C. Anelli, A. Baden, O. Baron, A. Belloni, B. Calvert, S.C. Eno, Y. Feng, C. Ferraioli, N.J. Hadley, S. Jabeen, G.Y. Jeng, R.G. Kellogg, J. Kunkle, A.C. Mignerey, F. Ricci-Tam, Y.H. Shin, A. Skuja, S.C. Tonwar

Massachusetts Institute of Technology, Cambridge, USA

D. Abercrombie, B. Allen, V. Azzolini, R. Barbieri, A. Baty, R. Bi, S. Brandt, W. Busza, I.A. Cali, M. D'Alfonso, Z. Demiragli, G. Gomez Ceballos, M. Goncharov, D. Hsu, M. Hu, Y. Iiyama, G.M. Innocenti, M. Klute, D. Kovalskyi, Y.S. Lai, Y.-J. Lee, A. Levin, P.D. Luckey, B. Maier, A.C. Marini, C. Mcginn, C. Mironov, S. Narayanan, X. Niu, C. Paus, C. Roland, G. Roland, J. Salfeld-Nebgen, G.S.F. Stephans, K. Tatar, D. Velicanu, J. Wang, T.W. Wang, B. Wyslouch

University of Minnesota, Minneapolis, USA

A.C. Benvenuti, R.M. Chatterjee, A. Evans, P. Hansen, J. Hiltbrand, S. Kalafut, Y. Kubota, Z. Lesko, J. Mans, S. Nourbakhsh, N. Ruckstuhl, R. Rusack, J. Turkewitz, M.A. Wadud

University of Mississippi, Oxford, USA

J.G. Acosta, S. Oliveros

University of Nebraska-Lincoln, Lincoln, USA

E. Avdeeva, K. Bloom, D.R. Claes, C. Fangmeier, R. Gonzalez Suarez, R. Kamalieddin, I. Kravchenko, J. Monroy, J.E. Siado, G.R. Snow, B. Stieger

State University of New York at Buffalo, Buffalo, USA

J. Dolen, A. Godshalk, C. Harrington, I. Iashvili, D. Nguyen, A. Parker, S. Rappoccio, B. Roozbahani

Northeastern University, Boston, USA

G. Alverson, E. Barberis, A. Hortiangtham, A. Massironi, D.M. Morse, T. Orimoto, R. Teixeira De Lima, D. Trocino, D. Wood

Northwestern University, Evanston, USA

S. Bhattacharya, O. Charaf, K.A. Hahn, N. Mucia, N. Odell, B. Pollack, M.H. Schmitt, K. Sung, M. Trovato, M. Velasco

University of Notre Dame, Notre Dame, USA

N. Dev, M. Hildreth, K. Hurtado Anampa, C. Jessop, D.J. Karmgard, N. Kellams, K. Lannon, N. Loukas, N. Marinelli, F. Meng, C. Mueller, Y. Musienko³⁶, M. Planer, A. Reinsvold, R. Ruchti, G. Smith, S. Taroni, M. Wayne, M. Wolf, A. Woodard

The Ohio State University, Columbus, USA

J. Alimena, L. Antonelli, B. Bylsma, L.S. Durkin, S. Flowers, B. Francis, A. Hart, C. Hill, W. Ji, B. Liu, W. Luo, D. Puigh, B.L. Winer, H.W. Wulsin

Princeton University, Princeton, USA

S. Cooperstein, O. Driga, P. Elmer, J. Hardenbrook, P. Hebda, S. Higginbotham, D. Lange, J. Luo, D. Marlow, K. Mei, I. Ojalvo, J. Olsen, C. Palmer, P. Piroué, D. Stickland, C. Tully

University of Puerto Rico, Mayaguez, USA

S. Malik, S. Norberg

Purdue University, West Lafayette, USA

A. Barker, V.E. Barnes, S. Das, S. Folgueras, L. Gutay, M.K. Jha, M. Jones, A.W. Jung, A. Khatiwada, D.H. Miller, N. Neumeister, C.C. Peng, H. Qiu, J.F. Schulte, J. Sun, F. Wang, W. Xie

Purdue University Northwest, Hammond, USA

T. Cheng, N. Parashar, J. Stupak

Rice University, Houston, USA

A. Adair, Z. Chen, K.M. Ecklund, S. Freed, F.J.M. Geurts, M. Guilbaud, M. Kilpatrick, W. Li, B. Michlin, M. Northup, B.P. Padley, J. Roberts, J. Rorie, W. Shi, Z. Tu, J. Zabel, A. Zhang

University of Rochester, Rochester, USA

A. Bodek, P. de Barbaro, R. Demina, Y.t. Duh, T. Ferbel, M. Galanti, A. Garcia-Bellido, J. Han, O. Hindrichs, A. Khukhunaishvili, K.H. Lo, P. Tan, M. Verzetti

The Rockefeller University, New York, USA

R. Ciesielski, K. Goulianos, C. Mesropian

Rutgers, The State University of New Jersey, Piscataway, USA

A. Agapitos, J.P. Chou, Y. Gershtein, T.A. Gómez Espinosa, E. Halkiadakis, M. Heindl, E. Hughes, S. Kaplan, R. Kunnawalkam Elayavalli, S. Kyriacou, A. Lath, R. Montalvo, K. Nash, M. Osherson, H. Saka, S. Salur, S. Schnetzer, D. Sheffield, S. Somalwar, R. Stone, S. Thomas, P. Thomassen, M. Walker

University of Tennessee, Knoxville, USA

A.G. Delannoy, M. Foerster, J. Heideman, G. Riley, K. Rose, S. Spanier, K. Thapa

Texas A&M University, College Station, USA

O. Bouhali⁶⁹, A. Castaneda Hernandez⁶⁹, A. Celik, M. Dalchenko, M. De Mattia, A. Delgado, S. Dildick, R. Eusebi, J. Gilmore, T. Huang, T. Kamon⁷⁰, R. Mueller, Y. Pakhotin, R. Patel, A. Perloff, L. Perniè, D. Rathjens, A. Safonov, A. Tatarinov, K.A. Ulmer

Texas Tech University, Lubbock, USA

N. Akchurin, J. Damgov, F. De Guio, P.R. Duderu, J. Faulkner, E. Gurpinar, S. Kunori, K. Lamichhane, S.W. Lee, T. Libeiro, T. Mengke, S. Muthumuni, T. Peltola, S. Undleeb, I. Volobouev, Z. Wang

Vanderbilt University, Nashville, USA

S. Greene, A. Gurrola, R. Janjam, W. Johns, C. Maguire, A. Melo, H. Ni, K. Padeken, P. Sheldon, S. Tuo, J. Velkovska, Q. Xu

University of Virginia, Charlottesville, USA

M.W. Arenton, P. Barria, B. Cox, R. Hirosky, M. Joyce, A. Ledovskoy, H. Li, C. Neu, T. Sinthuprasith, Y. Wang, E. Wolfe, F. Xia

Wayne State University, Detroit, USA

R. Harr, P.E. Karchin, N. Poudyal, J. Sturdy, P. Thapa, S. Zaleski

University of Wisconsin - Madison, Madison, WI, USA

M. Brodski, J. Buchanan, C. Caillol, S. Dasu, L. Dodd, S. Duric, B. Gomber, M. Grothe, M. Herndon, A. Hervé, U. Hussain, P. Klabbers, A. Lanaro, A. Levine, K. Long, R. Loveless, G. Polese, T. Ruggles, A. Savin, N. Smith, W.H. Smith, D. Taylor, N. Woods

†: Deceased

1: Also at Vienna University of Technology, Vienna, Austria

2: Also at State Key Laboratory of Nuclear Physics and Technology, Peking University, Beijing, China

3: Also at IRFU, CEA, Université Paris-Saclay, Gif-sur-Yvette, France

4: Also at Universidade Estadual de Campinas, Campinas, Brazil

5: Also at Universidade Federal de Pelotas, Pelotas, Brazil

6: Also at Université Libre de Bruxelles, Bruxelles, Belgium

7: Also at Institute for Theoretical and Experimental Physics, Moscow, Russia

8: Also at Joint Institute for Nuclear Research, Dubna, Russia

9: Also at Suez University, Suez, Egypt

10: Now at British University in Egypt, Cairo, Egypt

11: Also at Fayoum University, El-Fayoum, Egypt

12: Now at Helwan University, Cairo, Egypt

13: Also at Université de Haute Alsace, Mulhouse, France

14: Also at Skobeltsyn Institute of Nuclear Physics, Lomonosov Moscow State University, Moscow, Russia

15: Also at CERN, European Organization for Nuclear Research, Geneva, Switzerland

16: Also at RWTH Aachen University, III. Physikalisches Institut A, Aachen, Germany

17: Also at University of Hamburg, Hamburg, Germany

18: Also at Brandenburg University of Technology, Cottbus, Germany

19: Also at MTA-ELTE Lendület CMS Particle and Nuclear Physics Group, Eötvös Loránd University, Budapest, Hungary

20: Also at Institute of Nuclear Research ATOMKI, Debrecen, Hungary

21: Also at Institute of Physics, University of Debrecen, Debrecen, Hungary

22: Also at Indian Institute of Technology Bhubaneswar, Bhubaneswar, India

23: Also at Institute of Physics, Bhubaneswar, India

24: Also at University of Visva-Bharati, Santiniketan, India

25: Also at University of Ruhuna, Matara, Sri Lanka

26: Also at Isfahan University of Technology, Isfahan, Iran

27: Also at Yazd University, Yazd, Iran

28: Also at Plasma Physics Research Center, Science and Research Branch, Islamic Azad University, Tehran, Iran

29: Also at Università degli Studi di Siena, Siena, Italy

30: Also at INFN Sezione di Milano-Bicocca; Università di Milano-Bicocca, Milano, Italy

31: Also at Purdue University, West Lafayette, USA

32: Also at International Islamic University of Malaysia, Kuala Lumpur, Malaysia

33: Also at Malaysian Nuclear Agency, MOSTI, Kajang, Malaysia

34: Also at Consejo Nacional de Ciencia y Tecnología, Mexico city, Mexico

35: Also at Warsaw University of Technology, Institute of Electronic Systems, Warsaw, Poland

36: Also at Institute for Nuclear Research, Moscow, Russia

37: Now at National Research Nuclear University 'Moscow Engineering Physics

Institute' (MEPhI), Moscow, Russia

38: Also at St. Petersburg State Polytechnical University, St. Petersburg, Russia

39: Also at University of Florida, Gainesville, USA

40: Also at P.N. Lebedev Physical Institute, Moscow, Russia

41: Also at California Institute of Technology, Pasadena, USA

42: Also at Budker Institute of Nuclear Physics, Novosibirsk, Russia

43: Also at Faculty of Physics, University of Belgrade, Belgrade, Serbia

44: Also at University of Belgrade, Faculty of Physics and Vinca Institute of Nuclear Sciences, Belgrade, Serbia

45: Also at Scuola Normale e Sezione dell'INFN, Pisa, Italy

46: Also at National and Kapodistrian University of Athens, Athens, Greece

47: Also at Riga Technical University, Riga, Latvia

48: Also at Universität Zürich, Zurich, Switzerland

49: Also at Stefan Meyer Institute for Subatomic Physics (SMI), Vienna, Austria

50: Also at Gaziosmanpasa University, Tokat, Turkey

51: Also at Istanbul Aydin University, Istanbul, Turkey

52: Also at Mersin University, Mersin, Turkey

53: Also at Cag University, Mersin, Turkey

54: Also at Piri Reis University, Istanbul, Turkey

55: Also at Izmir Institute of Technology, Izmir, Turkey

56: Also at Necmettin Erbakan University, Konya, Turkey

57: Also at Marmara University, Istanbul, Turkey

58: Also at Kafkas University, Kars, Turkey

59: Also at Istanbul Bilgi University, Istanbul, Turkey

60: Also at Rutherford Appleton Laboratory, Didcot, United Kingdom

61: Also at School of Physics and Astronomy, University of Southampton, Southampton, United Kingdom

62: Also at Instituto de Astrofísica de Canarias, La Laguna, Spain

63: Also at Utah Valley University, Orem, USA

64: Also at Beykent University, Istanbul, Turkey

65: Also at Bingol University, Bingol, Turkey

66: Also at Erzincan University, Erzincan, Turkey

67: Also at Sinop University, Sinop, Turkey

68: Also at Mimar Sinan University, Istanbul, Istanbul, Turkey

69: Also at Texas A&M University at Qatar, Doha, Qatar

70: Also at Kyungpook National University, Daegu, Korea